The homogenized instrumental seismic catalog (HORUS) of Italy from 1960 to present

Seismological Research Letters

The HOmogenized instRUmental Seismic catalog (HORUS) of Italy from 1960 to present

--Manuscript Draft--

Manuscript Number:	SRL-D-20-00148R3
Full Title:	The HOmogenized instRUmental Seismic catalog (HORUS) of Italy from 1960 to present
Article Type:	Article - Regular Section
Corresponding Author:	Barbara Lolli, Ph.D. Istituto Nazionale di Geofisica e Vulcanologia Bologna, ITALY
Corresponding Author Secondary Information:	
Corresponding Author's Institution:	Istituto Nazionale di Geofisica e Vulcanologia
Corresponding Author's Secondary Institution:	
First Author:	Barbara Lolli, Ph.D.
First Author Secondary Information:	
Order of Authors:	Barbara Lolli, Ph.D.
	Daniele Randazzo, Dr.
	Gianfranco Vannucci, Ph.D.
	Paolo Gasperini, Prof.
Order of Authors Secondary Information:	
Manuscript Region of Origin:	ITALY
Abstract:	We implemented an automatic procedure to update in near real-time (daily to hourly) a homogeneous catalog of Italian instrumental seismicity to be used for forecasting experiments and other statistical analyses. The magnitudes of all events are homogeneously revalued so that to be consistent with Mw standard estimates made by the Global CMT project. For the time interval from 1960 to 15 April 2005 it is obtained by merging catalogs and online resources available for the Italian area and homogenizing all magnitudes to Mw according to empirical relationships computed using the Chi Square Regression method which properly consider the uncertainties of both variables. From 16 April 2005 to present, an automatic procedure periodically downloads the data of the on-line bulletin of the Istituto Nazionale di Geofisica e Vulcanologia (INGV) and of online Moment Tensor catalogs from respective websites, merges the different sources and applies traditional magnitude conversions to Mw. The final catalog is provided on a web site for public dissemination.
Suggested Reviewers:	
Opposed Reviewers:	

The HOmogenized instRUmental Seismic catalog (HORUS) of Italy from 1960 to present

Barbara Lolli[1]*, Daniele Randazzo[1], Gianfranco Vannucci[1] and Paolo Gasperini[2,1]

[1]Istituto Nazionale di Geofisica e Vulcanologia, Sezione di Bologna

[2]Dipartimento di Fisica e Astronomia, Università di Bologna

***Corresponding author: barbara.lolli@ingv.it**

Abstract

We implemented an automatic procedure to update in near real-time (daily to hourly) a homogeneous catalog of Italian instrumental seismicity to be used for forecasting experiments and other statistical analyses. The magnitudes of all events are homogeneously revalued so that to be consistent with Mw standard estimates made by the Global CMT project. For the time interval from 1960 to 15 April 2005 it is obtained by merging catalogs and online resources available for the Italian area and homogenizing all magnitudes to Mw according to empirical relationships computed using the Chi Square Regression method which properly consider the uncertainties of both variables. From 16 April 2005 to present, an automatic procedure periodically downloads the data of the on-line bulletin of the Istituto Nazionale di Geofisica e Vulcanologia (INGV) and of online Moment Tensor catalogs from respective websites, merges the different sources and applies traditional magnitude conversions to Mw. The final catalog is provided on a web site for public dissemination.

Introduction

Instrumental magnitudes of Italian earthquakes were determined in the last six decades according to different criteria in different time intervals (see Gasperini et al., 2013a, and Lolli et al., 2018 for an overview). In the last few years, we calibrated conversion relationships between various types of traditional magnitudes (ML, Md, Ms, mb) and moment magnitude Mw (Lolli and Gasperini, 2012, Gasperini et al., 2012, 2013a, 2013b, Lolli et al., 2014, 2015a, 2018) in order to obtain a homogeneous catalog of Italian earthquakes with magnitudes calibrated to Mw. Such homogenized magnitudes were considered for the compilation of the Catalogo Parametrico dei Terremoti Italiani version 2015 (CPTI15, Rovida et al., 2020) used in the latest revaluation of Italian seismic hazard map currently in progress. We also provided successive updates of the catalog to various national and international research groups involved in the statistical analysis of Italian seismicity and seismic hazard assessment (e.g. Gulia et al., 2016, 2018, Akinci et al., 2018, Fang et al., 2019, Gulia and Wiemer, 2019, Stallone and Marzocchi, 2019). Moreover, the occurrence of the 2016-2017 seismic sequence in Central Italy (Chiaraluce et al., 2017) evidenced the need of implementing an automatic procedure for updating the homogeneous catalog in near-real-time for monitoring and forecasting the time evolution of seismic sequences.

In our previous works, the conversion equations were all computed using datasets collected before 2011, hence their applicability to the subsequent years has to be verified. Moreover, the new global dataset of Mw from moment tensor inversion, made available by the Geo Forschungs Zentrum Potsdam (GFZP, see data and resource section) since 2011, must be calibrated before to being merged with other datasets.

In this work we describe the implementation of an automatic procedure for building and continuously updating the HOmogenized instRUmental Seismic catalog (HORUS) of the Italian area. Such procedure performs a) the downloading of hypocentral and magnitude data from the

Italian Seismological Instrumental and parametric Database (ISIDe[1]) of the Istituto Nazionale di Geofisica e Vulcanologia (INGV) and of Mw data from on-line moment tensor catalogs available for the Italian and Euromediterranean area; b) the matching of events of ISIDe with those of moment tensor catalogs, based on temporal and spatial criteria; c) the computation of Mw proxies from ML and Md according to Gasperini et al. (2013a) and their merging with true Mw estimates from moment tensor catalogs homogenized according to Gasperini et al. (2012); d) the assembly of the different sections of the catalog from 1960 to present; f) the copying of the homogeneous catalog on a publicly accessible web site.

We also redo all the calibrations of ML and Md magnitudes to Mw according to Gasperini et al. (2013a), by including data from 2011 to 2018 and also calibrate the Mw from the MT catalog of GFZP according to Gasperini et al. (2012). Finally, we estimate the magnitudes of completeness in the most recent part of the catalog.

Calibration of Mw datasets

Gasperini et al. (2012) calibrated five different datasets of true Mw determined by moment tensors inversion (GCMT, NEIC, RCMT, ETHZ and TDMT, see Data and resource section) at the Global, Euro-Mediterranean and Italian scale, using error-in-variables regression methods (Fuller, 1987, Stromeyer et al., 2004, Castellaro et al., 2006). They found that in general various datasets scale 1:1 with each other but some of them differ by average offsets. Gasperini et al. (2012) also found that the GCMT dataset, which is the first and more comprehensive collection of Mw at the global scale, tends to slightly overestimate Mw<5.4 while NEIC dataset tends to underestimate Mw>7 and then suggested to discard GCMT estimates if other datasets provide Mw<5.4 as well as to discard NEIC estimates if other datasets provide Mw>7.0 for the same earthquake. For the Italian

[1] In the ancient Egypt mythology Horus was the son of goddess Isis (Iside in Italian)

and Euro-Mediterranean areas, Gasperini et al. (2012) suggested to apply offset corrections of +0.05 to NEIC, -0.05 to ETHZ, +0.20 to TDMT, and none to RCMT before merging them with GCMT.

Gasperini et al. (2012) also estimated the uncertainties of Mw by considering the mean squared deviations σ_d between corrected Mw (after the application of offsets with respect to GCMT) from different MT datasets. They found $\sigma_d \cong 0.10$ magnitude units (m.u.) between any pair of datasets among GCMT, NEIC, ETHZ and RCMT and $\sigma_d \cong 0.15$ m.u. between TDMT and other datasets (Table 1). Hence they inferred that the uncertainties of Mw from GCMT, NEIC, ETHZ and RCMT were about $0.10/\sqrt{2} \cong 0.07$ m.u. and the uncertainty of Mw from TDMT were $\sqrt{0.15^2 - 0.07^2} \cong$ 0.13 m.u. Gasperini et al. (2013a) argued later that for GCMT estimates made before 1995, when the global broadband seismometric network was relatively coarse and a direct comparison with other datasets was not possible, an uncertainty of 0.10 m.u. is more appropriate.

When more than one Mw estimate is available from different datasets, Gasperini et al. (2012) suggested to compute the average of available (corrected) estimates, weighted by the inverse of the respective variance. In such cases, Gasperini et al. (2012) also proposed to assign to the computed average Mw a fixed uncertainty of 0.07 m.u. rather than the weighted mean uncertainty (corresponding to the square root of the inverse of the sum of weights), because the waveform data used by different datasets for the same earthquake mostly come from common stations and then the computed Mw's are not fully independent with each other. All average Mw estimates and their uncertainties are collected in an Integrated Moment Tensor catalog (IMT) that can be used as reference dataset for comparison with other kinds of magnitude.

The time interval analyzed by Gasperini et al. (2012) ends in 2010, then in the present work we verify all calibrations also including the data from 2011 to 2018. In such recalibration, we obviously do not consider the ETHZ dataset, discontinued in 2006, and the NEIC dataset,

96 discontinued in 2010. Moreover, we also calibrate the global Mw dataset of GFZP that was not
97 considered by Gasperini et al. (2012) because it was made available only since 2011.
98 We follow the same procedure adopted by Gasperini et al. (2012) based on linear Chi Square
99 regressions (CSQ, Stromeyer et al., 2004) between Mw from all pairs of datasets. CSQ accounts
100 for the uncertainty of both the dependent and independent variable and was demonstrated by Lolli
101 and Gasperini (2012) to be equivalent to the so called General Orthogonal Regression (GOR)
102 method (Fuller, 1987, Castellaro et al., 2006) when only the variance ratio is known. More recently
103 Das et al. (2014) proposed a modification of the method of Fuller (1987) but a comparison with
104 other methods by Gasperini et al. (2015) demonstrated that it has not to be used in magnitude
105 conversions.
106 As the GCMT is the first and most comprehensive collection of Mw at the global scale, we assume
107 it as a reference and calibrate all other datasets with respect to it. This does not mean that we are
108 certain that Mw estimated made by GCMT are the most accurate in the physical sense. However,
109 we believe that it is rather reasonable that it is so because the GCMT moment tensor inversion
110 procedure mainly employs very long period waves (with periods T=100-200 s) which are scarcely
111 influenced by seismic wave attenuation heterogeneities in the crust and the lithosphere. Hence, its
112 absolute calibration should be more accurate than that of other datasets (e.g. TDMT) employing
113 shorter period waves which are much more influenced by the heterogeneities of lithospheric
114 attenuation structure.
115 To compute CSQ linear regressions, we assume that the uncertainties of Mw estimates made by
116 different MT catalogs are the same for all earthquakes of any datasets and then that the variance
117 ratio is $\eta = 1$ (see Fuller, 1987) for all pairs of datasets. This assumption is consistent with the
118 evidence, noted above, that regression mean squared deviations σ_d between most pairs of datasets
119 computed by Gasperini et al. (2012) are very close with each other.

Following Gasperini et al. (2012), we verify if the computed regression slope differs significantly from 1 using the Student's t-test. If this occurs, Mw would need to be converted using the regressed linear law before to be merged with other estimates. If otherwise the Student's t-test provides a significance level larger than the standard critical threshold of 5% we can assume that the two datasets scale 1:1 with each other. In such case we compare the mean difference between Mw estimates for common earthquakes with the standard deviation of the mean difference (that is the sample standard deviation divided by the square root of the number of data pairs). If such average difference significantly differs from 0 based on the Student's t-test, a fixed offset has to be applied before merging such dataset with the other ones.

The results of the comparison of RCMT and TDMT with GCMT, for the period 2011-2018 (Tables 2 and 3), for the Italian (ITA) and Euro-Mediterranean (MED) areas, substantially confirm the findings of Gasperini et al. (2012) for the period before 2011. In fact, both RCMT and TDMT scale 1:1 with GCMT when Mw<5.4 data are not included in the comparison and the offsets Δ are about 0 for RCMT and about +0.20 m.u. for TDMT. Actually, for the linear relations between GCMT and TDMT in the Italian area (ITA), the Student's t-test would allow to reject the H_0 hypothesis $\beta=1$ with s.l. <0.05 but such inference is anyhow weak because the dataset is very small (only 6 data pairs).

In Table 4 we can see that even for GFZP, the significant scaling disagreement with respect to GCMT observed when using all data (Fig. 1a) disappears, for the Italian (ITA) and Euro-Mediterranean (MED) areas, when the data with Mw GFZP <5.4 are discarded (Table 4). At the global scale (GBL), the null hypothesis H_0:$\beta=1$ can still be rejected with s.l.<0.03 (Fig. 1b) but the estimated coefficient (β=1.005) is so close to 1 that its use in place of 1 in conversion equations would produce almost negligible differences in converted magnitudes (of the order of 0.01 m.u.). Then, even in this case, we can conclude that above Mw 5.4, GCMT and GFZP datasets generally

144 scale 1:1 with each other. We can note however that Mw from GFZP above 5.4 slightly
145 underestimates those from GCMT of about 0.05 m.u. Hence to merge GFZP with GCMT and other
146 datasets we will apply a positive offset correction of 0.05 m.u.
147 Concerning the uncertainties, the same analysis made by Gasperini et al. (2012) on the data from
148 2011 to 2018 (Table 5) now indicates mean squared deviations $\sigma_d \cong 0.10$ m.u. between almost
149 every pair of datasets (among GCMT, RCMT, GFZP and TDMT). Hence, we can conclude that
150 starting from 2011, an uncertainty of 0.07 m.u. can be assumed for all datasets, TDMT and GFZP
151 included.
152
153 **Recalibration of ISIDe magnitudes**
154 Before proceeding with the calibration of ISIDe magnitudes for the period 2011-2018 we must
155 mention that, starting from May 2012, the public domain software Earthworm (Johnson et al.,
156 1995), for real-time earthquake detection and location, replaced a former custom earthquake
157 location software used at the INGV until that time. This change implied some variations in the
158 informational content provided by ISIDe. In particular the duration magnitude Md, which
159 previously was computed using the Console et al. (1987) formula for most earthquakes, was now
160 provided only for a small portion of them (see in Table 6 that since 1 May 2012, Md is provided
161 for about 7% of earthquakes versus about 90% before). This is a pity because Gasperini et al.
162 (2013a) showed that the weighted average of ML and Md proxies is a more accurate and stable
163 Mw estimator than the ML proxy alone and hence has to be preferred for building a homogeneous
164 catalog.
165 In Table 6, we also show that before 1 May 2012, only 46 Md<1.0 (about 0.1% of the total) were
166 provided by ISIDe, whereas starting from such date to 2018 they are 2817 (about 17.5% of the
167 total number of Md). This suggests that some changes had occurred in the method of computing

Md starting more or less from the date of the migration to Earthworm. We investigated such question by comparing in Fig. 2 the plots of ML-Md pairs before and after 1 May 2012. We can note that the data cloud for the period since 1 May 2012 (crosses) appears shifted down (toward smaller Md) of about 0.5 m.u. with respect to the previous period (circles).

To further investigate this point, in Fig. 3 and in the second column of Table S1 of the supplemental material we show the average differences between the Mw proxies computed from ML and Md using the relationships developed by Gasperini et al. (2013a) in different time intervals. For all earthquakes occurred before 2011 (for which the above cited conversion formulas were computed) and in year 2011, such average difference is close to 0, whereas it is definitely negative in the following years. In particular, in 2012 the average difference is -0.17 m.u. and then, starting from 2013, it ranges from -0.7 to -0.9 m.u. In Fig. 3 and in the third column of Table S1 of the supplemental material, we also show that adding a positive correction of 0.45 magnitude units (m.u.) to Md, the average difference between the Mw proxies computed from ML and Md becomes close to 0 for years since 2013. Based on such evidences, we can argue that, about starting from 2013, an empirical correction of -0.4/-0.5 m.u. had possibly been applied to Md computed by the formula of Console et al. (1987). The possible motivation of such correction might have been that to make the raw Md values closer to ML. In fact, in Fig. 3 and in the last column of Table S1 of the supplemental material we show that the average absolute difference between ISIDe ML and Md was about 0.4-0.5 m.u. up to 2012 and reduces to about 0.0-0.2 m.u. starting from 2013. A more detailed analysis indicates that the numbers of Md<1.0 definitely increase (from about ten to several tens per month) starting from April 2013.

Note that a direct calibration of Md by a regression with Mw is not possible for the period since April 2013 because there are no data pairs available with both Md and Mw. Even the indirect calibration of Md with respect to ML, as done by Gasperini et al. (2013a), is poorly constrained

192 owing to the definitely lower number of data. Hence, to convert Md to Mw from April 2013 to
193 present, we will continue to use the relation obtained by Gasperini et al. (2013a) but first applying
194 an empirical offset correction of +0.45 m.u. to Md. Such value of the Md correction is computed
195 so that the average difference from April 2013 to 2018, between the Mw proxies from ML and Md
196 almost vanishes (see Table. S1 of supplemental material).
197 To calibrate ML with respect to Mw, we adopt the same procedure followed by Gasperini et al.
198 (2013a), which consists in estimating CSQ regressions (Stromeyer et al., 2004) of Mw as a function
199 of ML. For the dependent variable Mw, we assume the uncertainty $\sigma_{Mw} = 0.07$ as described in
200 section Recalibration of true Mw datasets and then adjust the uncertainty of independent variable
201 ML (σ_{ML}) so that to make the a-priori variance of the regression (Stromeyer et al., 2004, Lolli and
202 Gasperini, 2012)

$$\sigma^2_{a-priori} = \sigma^2_{\mathrm{Mw}} + \beta^2 \sigma^2_{ML} \tag{1}$$

203 to coincide with the empirical variance estimated from regression residuals

$$\sigma^2_{empirical} = \frac{1}{N-2} \sum_{1=1}^{N} (\mathrm{Mw}_i - \alpha - \beta \mathrm{ML}_i)^2 \tag{2}$$

204 where α and β are the linear regression intercept and coefficient (slope) respectively and N is the
205 number of Mw-ML data pairs used for the regression. By equating the two variances, we can infer
206 an approximate estimate of the uncertainty of ML as

$$\hat{\sigma}_{\mathrm{ML}} \approx \frac{1}{\beta} \sqrt{\frac{1}{N-2} \left[\sum_{1=1}^{N} (\mathrm{Mw}_i - \alpha - \beta \mathrm{ML}_i)^2 \right] - \sigma^2_{Mw}} \tag{3}$$

207 As varying σ_{ML} may vary the regression parameters and then the a-priori and empirical
208 standard deviations, some iterations are required to make $\sigma^2_{a-priori}$ and $\sigma^2_{rempirical}$ to
209 coincide with each other.

In Table 7 we report the final $\sigma_{empirical}$, the Mw average uncertainty ($\bar{\sigma}_{\mathrm{Mw}}$) and the estimated σ_{ML} for different time intervals. We can see a general tendency of σ_{ML} to slightly reducing for increasing time (from 0.17-0.18 before 2011 to 0.11-0.15 in the last years), which can be reasonably attributed to the continuous increase with time of the number of seismic stations computing the magnitudes in the INGV network. The only exception concerns the interval 2011-2012 in which we observe instead a definite increase of σ_{ML} (to 0.21 m.u.), which might be related to possible inconsistencies occurred in the first months of operation of Earthworms, just when a strong seismic sequence stroke Northern Italy starting from the 20 May 2012 mainshock (Mw=6.1).

We recomputed the calibration of ML with Mw even for the period from 2005 to 2010, already analyzed by Gasperini et al. (2013a), because we are aware of some retrospective changes applied to some datasets in the meantime (particularly RCMT and TDMT). Actually, we found 30 Mw-ML data pairs more than Gasperini et al. (2013a) but the result of the CSQ regression appears very similar to the previous paper (Table 8). The results of CSQ regressions for the whole period from 2011 to 2018 confirm the existence of a significant scaling disagreement between ML and Mw even if slightly smaller than that found in the previous period. We recall that Lolli et al. (2015b) argued that such significant scaling disagreement is possibly due to the use, for computing ML at INGV, of the distance correction formula of Hutton and Boore (1987), which is not particularly appropriate for the Italian region.

In Table 8, we also report the results of such regression analysis over intervals of two years from 2011 to 2019. Based on Student's t-test, the slope of the regression between Mw and ML is not significantly different from 1 in time intervals 2011-2012, 2013-2014 and 2017-2018 whereas it is significantly different and steeper than before 2011 in the time interval 2015-2016 when a strong earthquake sequence did occur in Central Italy. As for the largest event of such sequence

(Mw=6.6), occurred on 30 October 2016 at 6:40 UTC, the ML=6.1 appears definitely underestimated, we also tested if such underestimation could be the cause of the significant scaling disagreement we observed. We then recomputed the regression for periods 2011-2018 (Fig. 4) and 2015-2016 after eliminating such event. For both time intervals (2011-2018 and 2015-2016) however the scaling disagreement remains significant even if it slightly reduces.

The differences between the regression coefficient computed in various time intervals from 2011 to 2018 are relatively small excepting for the period 2011-2012 for which however we have relatively less data for computing the regression between Mw and ML. Moreover, the latter period was characterized by the entry into operation of the new acquisition system that might have somehow influenced the computation of magnitudes. We argue that for converting ML to Mw from 2011 to present it is reasonable to use a unique regression law and particularly that obtained for the entire period 2011-2018 without considering the largest earthquake with Mw=6.6 (Fig. 4). We also argue that, considering the very small difference between the regression coefficients determined in this work for the period 2005-2010 and those computed by Gasperini et al. (2013a), it is reasonable, even for maintain continuity with previous versions of the catalog, to continue to use the previously determined coefficients for converting ML to Mw from 2005 to 2010. In table 9 we summarize all the coefficients we finally adopted for magnitude conversions in the HORUS catalog.

Regularization of the frequency magnitude distribution

We already noted above that since May 2012, ISIDe does not anymore provide Md for the most of earthquakes and then the computation of Mw proxy is only based on the linear transformation of ML. As ISIDe provides ML magnitudes with only one decimal, the rounding error in conversion to Mw produces a strongly depleted class (Mw=2.2 in Fig. 5a) in the frequency magnitude

distribution (FMD). Waiting for INGV to provide (hopefully) more decimals in the future, we attempt the regularization of the FMD by generating randomly the second decimal of ML before computing the Mw proxies. We do that by simulating the same distribution that such decimal digit would have in real data by using the following transformation

$$\mathrm{M_r} = -\frac{1}{b}\log_{10}\left\{\mathrm{rand}(0,1)\left[10^{-b(\mathrm{M}+\Delta\mathrm{M}/2)} - 10^{-b(\mathrm{M}-\Delta\mathrm{M}/2)}\right]+10^{-b(\mathrm{M}-\Delta\mathrm{M}/2)}\right\} \quad (4)$$

Where M and Mr are the original and recomputed magnitudes respectively, ΔM =0.1 is the original data resolution and rand(0,1) is a uniform pseudo random variable in the range [0,1]. The result in Fig. 5b (using *b*=1) shows that the depleted class totally disappears. Note that after applying eq. (4) the *b*-value of the Gutenberg and Richter (1944) law (now on GR law) slightly but significantly decreases from 1.054±0.005 to 1.028±0.005.

Also note that in Fig. 6a, showing the same plot of Fig. 5a but for period from 16 April 2005 to 30 April 2012 (when Md was provided by ISIDe for the most of the earthquakes), no depleted classes are particularly evident because the averaging between ML and Md proxies naturally randomizes the second decimal digit. In this case the application of the same transformation of eq. (4) (Fig. 6b) slightly regularize the FMD but does not vary significantly the *b*-value (going from 0.976±0.008 to 0.987±0.008).

Since this regularization procedure might be questioned as it arbitrarily modifies the original data (even if very slightly), we will supply two versions of the HORUS catalog with uncorrected and corrected Mw proxies respectively.

Building the homogeneous catalog in near real-time

From 1960 to 1980 the homogeneous catalog corresponds to the supplemental material of Lolli et al. (2018) (see Data and resource section). From 1981 to 15 April 2005, it is obtained as the

combination of various data sources according to the compilation criteria and the conversion equations developed by Gasperini et al. (2013a). In particular the main sources of hypocentral and magnitude data are: from 1981 to 1996 the Catalogo Parametrico dei Terremoti Italiani (CSTI) version 1.1 (CSTI Working group, 2004), from 1997 to 2002 the Catalogo della Sismicità Italiana (CSI) version 1.1, compiled according to Castello et al. (2007), and from 2003 to 15 Apr 2005, the Bollettino Sismico Italiano (BSI) (see Data and Resources section). Such sources are integrated with available Mw's from the IMT. Such parts of the HORUS catalog are substantially static and in general do not require a near real-time update but only a periodic rebuilding in order to include possible retrospective corrections of the Mw from MT catalogs if any.

To build and maintain up to date the catalog from 16 April 2005 to present time, the ISIDe, GCMT, RCMT GFZP and TDMT websites are periodically queried to download their updated versions. Our present approach aims to maintain up to date the homogenized datasets at an hourly basis. Hence, every hour we access all sources for downloading the data of the last 24 hours so that to even account for possible updates of quick or preliminary determinations made in the last day. Daily, we download the data of the previous year and monthly the entire database. This time schedule represents a compromise between the opposing demands to promptly integrate in our database all possible data improvements made by various sources and to not load too much the data providers with heavy queries.

The data are downloaded automatically from respective providers (see Data and Resource section) by a process that sleeps on our server until different crontab times are reached. Such process is based on a suite of Python programs that send the queries to the various web-sites, wait for the completion and correctness of the answers and finally stores the downloaded data in a folder that is accessible to our conversion and homogenization procedure.

303 The latter consists of a suite of Fortran programs that we adapted from those we were running
304 manually when we prepared our papers on magnitude conversions (see above). All of them run
305 now in sequence unattended. First the downloaded datasets are converted into tab separated txt
306 files in a common custom format and are ordered chronologically. Then the files of various sources
307 of moment magnitudes are merged and common events are matched based on fixed time and
308 spatial intervals as described in Gasperini et al. (2012) for Mw catalogs and in Gasperini et al.
309 (2013) between ISIDe and Mw catalogs. The matching of new data is manually checked monthly
310 and in case of missed or wrong matching between earthquakes in the two catalogs the correct
311 matching is forced by setting specific exceptions in the matching code. The reference Mw for each
312 earthquake, computed as weighted average of available estimates corrected for offsets (Table 9),
313 is included in the Integrated Moment Tensor (IMT) catalog. The Mw's from the IMT catalog are
314 then merged and matched with the ISIDe Mw proxies computed from Md and ML using
315 coefficients shown in Table 9. In case a true Mw magnitude is available from the IMT dataset, the
316 ISIDe proxies are ignored. The unmatched IMT records are also added to the catalog and all
317 records are chronologically sorted. The resulting catalog from 16 April 2005 to (almost) present
318 time is added to the catalog from 1960 to 15 April 2005 computed according to Gasperini et al.
319 (2013) and Lolli et al. (2018) and then compressed in a zipped file (of about 9 Mbytes at present
320 time).
321
322 **Completeness of the homogenized catalog**
323 For the period up to 2010 the approximate magnitude completeness thresholds were determined
324 by Gasperini et al (2013a) and Lolli et al. (2018) as reported in Table 10. As the seismic network
325 coverage is poor in offshore areas and out of Italian boundaries, in such works as well in the present
326 one, the analysis of completeness is restricted to earthquakes located within the Italian mainland.

Several methods to assess the completeness of an instrumental catalog were proposed in the literature (e.g. Wiemer and Wyss, 2000, Cao and Gao, 2002, Woessner and Wiemer, 2005). They are all based on the comparison between the observed FMD and that predicted by the GR law fitted on the complete part of the dataset

$$\log_{10} N = a - b\mathrm{M} \quad (5)$$

where N is the number of earthquakes above a given magnitude M (cumulative GR) or within magnitude bins centered in M (non-cumulative GR) and a and b are empirical coefficients. It is easy to show that b has the same value for both the cumulative and non-cumulative distributions. Above the completeness magnitude threshold Mc, the observed FMD almost coincides with the GR law, whereas below it the two functions diverge and the GR law overestimates the observed FMD. This is the principle on which it is based the Maximum Curvature (MC) method (Wiemer and Wyss, 2000) which assess the Mc at the magnitude bin with the highest frequency of earthquakes in the non-cumulative FMD. As this simple approach tends to underestimate Mc, Woessner and Wiemer (2005) suggested to add a correction value (e.g. 0.2 m.u.) to the magnitude of bin with the highest frequency.

Such completeness assessment methods are aimed to provide a reliable estimate of Mc but are also designed to be fast and to not require manual operations. On a side such procedure guarantees the objectivity of the estimated Mc but on the other it might not capture peculiar characteristics of the real data distribution. In particular all automatic methods may fail when the real FMD is not perfectly linear even above Mc.

Following Gasperini et al. (2013a) and Lolli et al. (2014), we adopt an interactive (IN) approach based on the visual inspection of plots like those reported in Fig. 7a for the HORUS catalog from 16 Apr 2005 to 2019. The cumulative FMD (solid line) is plotted as the inverse ordering rank (from the largest to the smallest one) of each magnitude and the non-cumulative FMD (black

circles) as the number of earthquakes within bins of 0.1 m.u. as a function of the central magnitude of each bin. Both counts are normalized to the total duration (14.7 years) of the time interval so that they correspond to annual rates. We also plotted in Fig. 7a the GR lines (thin black) corresponding to the *b*-value computed according to the maximum likelihood method (Aki 1965) corrected for the data binning (Bender, 1983). The vertical dashed line indicates the estimated completeness magnitude threshold of the catalog (Mw = 1.8). In the upper-right inset we display the behavior of the completeness rate, defined as the ratio between observed and predicted rates with Mw≥Mmin. In the lower-left inset we show instead the *b*-value as a function of cut-off magnitude Mmin.

Such plots are implemented in a MS Excel worksheet in which we can vary the tentative Mc at wish, with automatic update of counts and plots. We assess the best completeness threshold Mc as the smaller magnitude starting from which the plot of *b*-value as a function of cutoff magnitude Mmin is relatively stable and there is a good correspondence between observed rates and those predicted by the GR law as evidenced by a completeness rate close to 100% on a magnitude range as wide as possible.

In Fig. 7a, we can see that both the cumulative and non-cumulative FMD for the entire HORUS catalog almost coincide with the fitted GR best lines with b=1.017±0.004 from the estimated Mc at Mw=1.8 to about Mw=4.0. From Mw=4.0 to Mw=5.0 the cumulative line slightly overestimates observations, from Mw=5.0 to Mw=5.5 the agreement of the line with the observations slightly improves, and at larger magnitudes the GR line definitely underestimate observations. This behavior is also reflected by the completeness rate displayed in the in upper right inset, which is close to 100% for Mw ranging from 1.8 to 4.0, about 90% from 4.0 to 5.5 and definitely larger than 100% at larger magnitudes. We also see in the lower left inset that the *b*-value is constant or anyhow lies within error bars over a range of cutoff magnitude Mmin from Mw=1.8 to Mw=6.0.

Note that if the completeness threshold were assessed by the corrected MC method (adding 0.2 m.u. to the magnitude bin with the maximum number of data in the non-cumulative FMD), both Mc and the *b*-value would have been definitely underestimated (1.4 and 0.924±0.003 respectively). We may argue that this poor performance of a method that proved to work well with many other datasets (Woessner and Wiemer, 2005), might be related to a spatial heterogeneity of the capability of Italian seismic network to detect and locate small earthquakes (Schorlemmer et al., 2010). We might also argue that, in the Italian region, the correction to apply to the maximum curvature magnitude to obtain Mc should be definitely larger than the usually adopted value of 0.2 m.u..

In Fig. 7b, we display the same plots for the preferred (default) magnitude Mp provided by ISIDe In this case the *b*-value above completeness (Mp=1.8) is slightly but significantly larger (*b*=1.064±0.004) than for the HORUS catalog. The behavior of *b*-value as a function of cutoff Mmin (lower left inset) shows more pronounced variations with respect to the HORUS catalog in Fig. 7a and the completeness rate (upper right inset) definitely decreases from about 100% for Mp<3.0 to about 80% around Mp=4.0. Note that Mp is chosen by INGV seismic network operators as one among ML, Md and the Mw computed by the TDMT method (Dreger et al., 2005) according to Scognamiglio et al. (2009). In case of deep events, the short period body wave magnitude (mb) provided by international observatories may be chosen.

In Fig. 8 and in Table S2 of supplemental material we report the Mc and *b*-value of HORUS, computed separately for all years from 2005 to 2019 by the IN approach (dark grey lines) and by the corrected MC method (light grey lines). In particular in Fig. 8a, the Mc assessed by the IN method (see the relevant plots in Figs. S1 to S15 of the supplemental material) generally decreases from 1.8 in 2005 to 1.3 in 2019, but clear increases can be noted in years 2008, 2012 and 2016. The Mc computed by the corrected MC method almost always underestimates the one by the IN approach and shows a more regular behavior without very large peaks. The underestimation is of

the order of 0.1 m.u. or less from 2005 to 2007 and from 2016 to 2019, of the order of 0.3-0.4 m.u. from 2008 to 2011 and from 2013 to 2015, and 0.9 m.u. in 2012. Correspondingly, the *b*-value computed using Mc from the MC method is slightly underestimated with respect to the IN method from 2005 to 2007, more significantly underestimated from 2008 to 2015, and almost the same from 2016 to 2019.

To better understand such anomalies, we also plotted in Fig. 8a (black lines), as an index of seismic activity in each year, the logarithm of the annual rate of earthquakes with Mw≥2.5. The black solid and black dashed lines refer to actually observed rates and to rates predicted by the GR law respectively. For years 2012 and 2016 we could argue that the increase of Mc be related to the difficulty of the seismic network to locate thousands of aftershocks in the weeks and months after the main shocks with Mw≥6 occurred in these years but for year 2008 the explanation is not obvious as no strong main shocks did occur in such year. Conversely a main shock, with Mw=6.3 occurred on 6 April 2009 close to the town of L'Aquila (Central Italy) but the Mc in 2009 would appear lower than in 2008. One possible explanation of such anomaly could be that after the L'Aquila main shock the seismic network has made every effort to process the shocks of the ongoing sequence but somehow neglecting previous time periods.

This is somehow confirmed by the monthly behavior of Mc and of seismic activity from September 2008 to April 2010 reported in Fig. 9 (see values in Table S3 of the supplemental material). We can note how IN Mc is particularly low (around 1.3-1.4) from May to November 2009 and even in April 2009, when the seismic activity was maximum, it is not higher than the average of previous months. Conversely it is definitely higher in December 2008 and December 2009 when the seismic activity was higher than average but anyhow definitely lower than in April 2009. The high activity in December 2008 is possibly related to the aftershocks of an earthquake with Mw=5.4 occurred near the town of Parma (Northern Italy) while that in December 2009 to a very productive and

422 damaging seismic sequence (with maximum magnitude 4.4) occurred in the north-western flank
423 of Mt. Etna volcano (eastern Sicily).
424 The same plot for year 2012 and neighboring months is displayed in Fig. 10 (see values in Table
425 S4 of the supplemental material). Here a IN Mc as high as 2.3, estimated for the entire year 2012,
426 is only observed in May and in June when the strong sequence in the Pianura Emiliana was very
427 active, whereas in other months, it ranges between 1.3 to 1.8. In this case, different from the 2008-
428 2009 period, it does not seem that that the strong effort made by the seismic network during the
429 sequence had influenced the previous time periods.
430 Finally, for 2016 displayed in Fig. 11 (see values in Table S5 of the supplemental material), the
431 largest increase of interactive Mc is in October when the largest main shock (Mw=6.6) of the
432 Central Italy sequence did occur. The increase to Mc=2 in January 2016 can also be explained by
433 a definite increase of the seismic activity related to a sequence in the Molise region. More in
434 general the efficiency of the seismic network appears to not being decreased significantly
435 notwithstanding the strong effort made during the Central Italy sequence.
436

437 **Concluding remarks**

438 We implemented an automatic procedure to build and update the Italian seismic catalog HORUS
439 with magnitude converted so that to be homogeneous with Mw estimated by the Global CMT
440 project (Dziewonki et al., 1981, Ekström et al, 2012). The time interval ranges from 1960 to present
441 time but the accuracy and the completeness vary considerably owing to the progressive
442 improvement of the Italian seismic detection network with time.
443 Hypocentral locations are taken as they are provided by the various sources without any
444 modification while the magnitudes are converted from different definitions by empirical linear

445 conversion relations derived by Chi Square regressions (Stromeyer et al., 2004), which properly
446 consider the uncertainty of both the dependent and independent variables.
447 One of the problems we encountered is the limited resolution of the magnitudes, which are
448 provided by INGV with only one decimal digit. When magnitudes are converted to Mw, this
449 generates a rounding error which depletes some magnitude classes. Up to 2012 this problem was
450 mitigated by the possibility to average the converted Mw proxy from both ML and Md.
451 Unfortunately, since the installation in May 2012 of the new acquisition system Earthworm
452 (Johnson et al, 1996) at INGV, Md magnitudes are not provided anymore for most earthquakes.
453 We hope that in the future INGV will decide to provide Md for all earthquakes because such
454 magnitude estimate, although less reliable than ML, provides anyhow additional information on
455 earthquake size, being based on different measured parameters. Hence the averaging of Mw
456 proxies from both ML and Md significantly improve the accuracy and the homogeneity of the final
457 magnitude (Gasperini et al., 2013a).
458 We also hope that in the future INGV will decide to provide magnitudes with two decimal digits
459 at least but in lack of that we were able to produce converted Mw proxies from ML only with no
460 depleted classes by generating the second decimal digit randomly with the same distribution of
461 real data, before to applying the magnitude conversion. As this implies an alteration of data that
462 might be questioned, we also provide an uncorrected version of the catalog.
463 The final HORUS catalog is provided as two tab-delimited text files (with uncorrected and
464 corrected Mw proxies respectively) included in a zip file (of about 17 Mbytes presently), which
465 can be freely downloaded from the web site horus.bo.ingv.it.
466 The file is updated about every hour with most recent data and almost completely rebuilt every
467 month. We check possible malfunctions of the procedure by comparing the latest version with the
468 preceding one and sending a mail to some of us if an excessive number of differences is found.

All successive versions of the input and output files are saved in different folders for tracing possible malfunctions.

The procedure is currently under beta test, hence we cannot guarantee the absolute correctness of the provided catalog. All feedbacks from users are welcomed by authors.

Data and resource section

Supplemental material for this article includes additional figures (from S1 to S15) and tables (from S1 to S5) useful to better describe methods and results.

The Italian Seismological Instrumental and parametric Database (ISIDe) of the Istituto Nazionale di Geofisica e Vulcanologia (INGV) from 2005 to present (ISIDe Working Group, 2007) is collected at http://webservices.ingv.it/ (last accessed April 2020).

The MT catalog of the Geo Forschungs Zentrum Potsdam (GFZP) from 2011 to present (Saul et al, 2011) is collected at http://geofon.gfz-potsdam.de/data/alerts/ (last accessed July 2020).

The European-Mediterranean Regional Centroid Moment Tensor (RCMT) catalog of INGV from 1997 to present (Pondrelli et al., 2002, 2011) is collected at http://rcmt2.bo.ingv.it/data/EuroMedCentrMomTensors.csv (last accessed April 2020) for definitive solutions and at http://autorcmt.bo.ingv.it/QRCMT-on-line/ (last accessed April 2020) for quick preliminary solutions. Other solutions available for earthquakes before 1997 are collected from webpages linked at http://rcmt2.bo.ingv.it (last accessed April 2020).

The Global Centroid Moment Tensor (GCMT) catalog from 1976 to present (Dziewonski et al., 1981, Ekström et al, 2012) is collected at https://www.globalcmt.org (last accessed April 2020). Other solutions available for particular datasets are collected at webpages linked at the same address.

The Time Domain Moment Tensor (TDMT) catalog of INGV (Dreger et al., 2005, Scognamiglio et al., 2009) from 2005 to present is collected at http://webservices.ingv.it/ (last accessed April 2020).

The MT catalog of the Eidgenössische Technische Hochschule Zürich (ETHZ) from 1999 to 2006 (Bernardi et al., 2004) was collected at http://www.seismo.ethz.ch/prod/tensors/mt_oldcat/index_EN (last accessed December 2012).

The MT catalog of the National Earthquake Information Center (NEIC) of the U.S. Geological Survey from 1980 to 2010 (Sipkin, 1994) was collected using http://earthquake.usgs.gov/earthquakes/ eqarchives/sopar/ (last accessed December 2012).

The homogeneous catalog of Italian Earthquakes from 1960 to 1980 according to Lolli et al. (2018) was collected at https://pubs.geoscienceworld.org/ssa/bssa/article/108/1/481/525362/?searchresult=1#supplementary-data (last accessed April 2020).

The *Catalogo Strumentale dei Terremoti Italiani* (CSTI) version 1.1 (CSTI Working group, 2003, 2004) from 1981 to 1996 is collected at https://emidius.mi.ingv.it/CSTI/Versione1_1/ (last accessed July 2020).

The *Catalogo della Sismicità Italiana* (CSI) version 1.1 from 1981 to 2002 (Castello et al, 2006) (only data since 1997 are considered), compiled according to Castello et al. (2007), is collected at http://csi.rm.ingv.it/ (last accessed April 2020).

The *Bollettino Sismico Italiano* (BSI) from 2003 to 2012 was collected at http://bollettinosismico.rm.ingv.it/ (last accessed April 2020).

Supplemental material includes additional figures and tables. Figures S1 to S15 show cumulative frequency-magnitude distribution of HORUS catalog for years from 2005 to 2019. Table S1 to S3 report numerical values plotted in Figures 98 to 10 of the main text.

Acknowledgements

The authors thank the editor and the referees for they criticisms that helped to improve the paper. This paper benefitted from funding provided by the Ministero dell'Istruzione, dell'Università e della Ricerca (MIUR) within the ambit of the FISR 2016 project (U.R. 41 Resp. B. Lolli).

References

Aki, K. (1965). Maximum likelihood estimate of b in the formula logN= a – b M and its confidence limits, Bull. Earthq. Res. Inst. Univ. Tokyo 43, 237–239.

Akinci, A., M. P. Moschetti, and M. Taroni (2018). Ensemble Smoothed Seismicity Models for the New Italian Probabilistic Seismic Hazard Map, Seism. Res. Lett., 89/4, 1277-1287, doi: 10.1785/0220180040.

Bender, B. (1983). Maximum likelihood estimation of b values for magnitude grouped data, Bull. Seismol. Soc. Am. 73, 831–851.

Bernardi, F., J. Braunmiller, U. Kradolfer, and D. Giardini (2004). Automatic regional moment tensor inversion in the European-Mediterranean region, Geophys. J. Int., 157, 703–716.

Cao, A., and S. S. Gao (2002). Temporal variation of seismic b-values be- neath northeastern Japan island arc, Geophys. Res. Lett. 29, no. 9, doi: 10.1029/2001GL013775.

Castellaro, S., F. Mulargia, and Y. Y. Kagan (2006). Regression problems for magnitudes, Geophys. J. Int. 165, 913–930.

Castello, B., G. Selvaggi, C. Chiarabba, and A. Amato (2006). CSI Catalogo della sismicità italiana 1981-2002, versione 1.1. INGV-CNT, Roma

546 Castello, B., M. Olivieri, and G. Selvaggi (2007). Local and duration magnitude determination for
547 the Italian Earthquake Catalog, 1981–2002, Bull. Seismol. Soc. Am. 97, 128–139.
548
549 Chiaraluce, L., R. Di Stefano, E. Tinti, L. Scognamiglio, M. Michele, E. Casarotti, M. Cattaneo,
550 P. De Gori, C. Chiarabba, G. Monachesi, A. Lombardi, L. Valoroso, D. Latorre, and S. Marzorati
551 (2017). The 2016 Central Italy Seismic Sequence: A First Look at the Mainshocks, Aftershocks,
552 and Source Models, Seism. Res. Lett., 88/3, 757-771, doi: 10.1785/0220160221.
553
554 Console, R., B. De Simoni, and A. Di Sanza (1989). Riesame della relazione magnitudo-distanza,
555 in Proc. VII Conference of the Gruppo Nazionale di Geofisica della Terra Solida (GNGTS), Rome,
556 30 November–2 December 1988, 51–61 (in Italian).
557
558 CSTI Working Group (2004). Catalogo strumentale dei terremoti Italiani dal 1981 al 1996,
559 Versione 1.1, https://emidius.mi.ingv.it/CSTI/Versione1_1/ (in Italian).
560
561 Das, R., H. R. Wason, and M. L. Sharma (2014). Unbiased estimation of moment magnitude from
562 body- and surface-wave magnitudes, Bull. Seismol. Soc. Am. 104, no. 4, 1802–2014, doi:
563 10.1785/0120130324.
564
565 Dreger, D. S., L. Gee, P. Lombard, M. H. Murray, and B. Romanowicz (2005). Rapid finite-source
566 analysis and near-fault strong ground motions: Application to the 2003 Mw 6.5 San Simeon and
567 2004 Mw 6.0 Parkfield earthquakes. Seismological Research Letters 76 (1), 40–48.
568

569 Dziewonski, A. M., T.-A. Chou, and J. Woodhouse (1981). Determination of earthquake source
570 parameters from waveform data for studies of global and regional seismicity, J. Geophys. Res. 86,
571 2825–2852.
572
573 Ekström, G., M. Nettles, and A. M. Dziewonski (2012). The global CMT project 2004-2010:
574 centroid-moment tensor solutions for 13,017 earthquakes, Phys. Earth planet. Inter., 200-201, 1-9,
575 doi: 10.1016/j.pepi.2012.04.002.
576
577 Fang, J., D. Zhou, L. M. Shekhtman, A. Shapira, R. Hofstetter, W. Marzocchi, Y. Ashkenazy, and
578 S. Havlin (2019). Possible origin of memory in earthquakes: Real catalogs and an epidemic-type
579 aftershock sequence model, Phys Rev., 99, 042210, doi: 10.1103/PhysRevE.99.042210.
580
581 Fuller, W. A. (1987). Measurement Error Models, John Wiley, New York, 440 pp.
582
583 Gasperini P., Lolli B., Vannucci G., Boschi E. (2012). A comparison of moment magnitude
584 estimates for the European–Mediterranean and Italian region, Geophys. J. Int., 190, 1733-1745,
585 doi: 10.1111/j.1365-246X.2012.05575.x.
586
587 Gasperini P., Lolli B. and Vannucci G. (2013a). Empirical Calibration of Local Magnitude Data
588 Sets Versus Moment Magnitude in Italy, Bull., Seism. Soc. Am., 103, 2227-2246, doi:
589 10.1785/0120120356.
590

Gasperini P., Lolli B. and Vannucci G. (2013b). Body-Wave Magnitude mb Is a Good Proxy of Moment Magnitude Mw for Small Earthquakes (mb < 4.5–5.0), Seism. Res. Lett., 84(6), 932-937, doi:10.1785/0220130105.

Gasperini, P., B. Lolli, and S. Castellaro (2015). Comparative Analysis of Regression Methods Used for Seismic Magnitude Conversions, Bull. Seism. Soc. Am., 105(3), 1787-1791, doi: 10.1785/0120150018.

Gulia L., T. Tormann, S. Wiemer, M. Herrmann, and S. Seif (2016). Short-term probabilistic earthquake risk assessment considering time-dependent b values, Geophys. Res. Lett., 43, doi:10.1002/2015GL066686.

Gulia, L., A. P. Rinaldi, T. Tormann, G. Vannucci, B. Enescu, and S. Wiemer (2018). The Effect of a Mainshock on the Size Distribution of the Aftershocks, Geophys/. Res. Lett.,24, 13277-13287, doi: 10.1029/2018GL080619.

Gulia, L, and S. Wiemer (2019). Real-time discrimination of earthquake foreshocks and aftershocks, Nature, 574, 193-199, doi: 10.1038/s41586-019-1606-4.

Gutenberg, B., and C. F. Richter (1944). Frequency of earthquakes in California, Bull Seism. Soc. Am., 34, 185-188.

Hutton, L. K., and M. Boore (1987). The ML scale in southern California, Bull. Seismol. Soc. Am. 77, 2074–2094.

ISIDe Working Group. (2007). Italian Seismological Instrumental and Parametric Database (ISIDe). Istituto Nazionale di Geofisica e Vulcanologia (INGV). doi: 10.13127/ISIDE.

Johnson, C. E., A. Bittenbinder, B. Bogaert, L. Dietz, and W. Kohler (1995). Earthworm: A flexible approach to seismic network processing, Incorporated Research Institutions for Seismology (IRIS) Newsletter 14, 1–4

Lolli B., and P. Gasperini (2012). A comparison among general orthogonal regression methods applied to earthquake magnitude conversions, Geophys. J. Int., 190, 1135-1151, doi: 10.1111/j.1365-246X.2012.05530.x.

Lolli, B., P. Gasperini, and G. Vannucci (2014). Empirical conversion between teleseismic magnitudes (mb andMs) and moment magnitude (Mw) at the Global, Euro-Mediterranean and Italian scale, Geophys. J. Int., 199, 805–828, doi: 10.1093/gji/ggu264.

Lolli, B., P. Gasperini, and G.Vannucci (2015a). Erratum: Empirical conversion between teleseismic magnitudes (mb andMs) and moment magnitude (Mw) at the Global, Euro-Mediterranean and Italian scale, Geophys. J. Int., 200, 199–199, doi: 10.1093/gji/ggu385.

Lolli, B., P. Gasperini, F. M Mele., and G. Vannucci (2015b). Recalibration of the Distance Correction Term for Local Magnitude (ML) Computations in Italy, Seism. Res. Lett., 85 (5), 1383-1392, doi: 10.1785/0220150020.

639 Lolli, B., P. Gasperini, and A. Rebez (2018). Homogenization in terms of Mw of local magnitudes
640 of Italian earthquakes occurred before 1981, Bull. Seism. Soc. Am., 108, No. 1, 481–492, doi:
641 10.1785/0120170114.
642
643 Pondrelli, S. , A. Morelli , G. Ekström, S. Mazza, E. Boschi, and A.M. Dziewonski (2002).
644 European-Mediterranean regional centroid- moment tensors: 1997–2000, Phys. Earth planet.
645 Inter., 130, 71– 101.
646
647 Pondrelli, S., S. Salimbeni, A. Morelli, G. Ekström, L. Postpischl, G. Vannucci, and E. Boschi
648 (2011). European–Mediterranean Regional Centroid Moment Tensor catalog: solutions for 2005–
649 2008, Phys. Earth planet. Inter., 185, 74–81.
650
651 Rovida, A., M. Locati, R. Camassi, B. Lolli, and P. Gasperini (2020), The Italian earthquake
652 catalogue CPTI15, Bull. Earth. Eng. (published online), doi: 10.1007/s10518-020-00818-y.
653
654 Saul, J., J. Becker, and W. Hanka (2011). Global moment tensor computation at GFZ Potsdam,
655 AGU Fall Meeting, Sn Francisco, USA, abstract ID. S51A-2202
656
657 Schorlemmer, D., F. Mele, and W. Marzocchi (2010). A completeness analysis of the National
658 Seismic Network of Italy, J. Geophys. Res., 115, B04308, doi:10.1029/2008JB006097.
659
660 Scognamiglio, L., Tinti, E. & Michelini, A., 2009. Real-time determination of seismic moment
661 tensor for the Italian region, Bull. seism. Soc. Am., 99, 2223–2242.
662

Stallone, A., and W. Marzocchi (2019). Features of Seismic Sequences Are Similar in Different Crustal Tectonic Regions, Bull. Seism. Soc. Am., 109/5, 1594-1604, doi: 10.1785/0120180175

Sipkin, S.A. (1994). Rapid determination of global moment-tensor solutions, Geophys. Res. Lett., 21(16), 1667–1670.

Stromeyer, D., G. Grünthal, and R. Wahlstroöm (2004). Chi-square regression for seismic strength parameter relations, and their uncertainties, with applications to an Mw based earthquake catalogue for central, northern and northwestern Europe, J. Seismol., 8(1), 143–153.

Wiemer, S., Wyss, M., 2000. Minimum magnitude of completeness in earthquake catalogs: examples from Alaska, the Western United States and Japan. Bull. Seismol. Soc. Am. 90, 859–869. https://doi.org/10.1785/0119990114.

Woessner, J., Wiemer, S., 2005. Assessing the quality of earthquake catalogues: estimating the magnitude of completeness and its uncertainty. Bull. Seismol. Soc. Am. 95, 684–698. https://doi.org/10.1785/0120040007.

Authors' addresses

Barbara Lolli

Istituto Nazionale di Geofisica e Vulcanologia, Sezione di Bologna, Via Donato Creti 12, 40128 Bologna, Italy, email: barbara.lolli@ingv.it

687 Daniele Randazzo
688 Istituto Nazionale di Geofisica e Vulcanologia, Sezione di Bologna, Via Donato Creti 12, 40128
689 Bologna, Italy, email: daniele.randazzo@ingv.it
690
691 Gianfranco Vannucci
692 Istituto Nazionale di Geofisica e Vulcanologia, Sezione di Bologna, Via Donato Creti 12, 40128
693 Bologna, Italy, email: gianfranco.vannucci@ingv.it
694
695 Paolo Gasperini
696 Dipartimento di Fisica e Astronomia, Università di Bologna, Viale Berti Pichat 6/2, 40127
697 Bologna, Italy, email: paolo.gasperini@unibo.it
698

Tables

Table 1 – Mean squared deviations σ_d between couples of corrected Mw taken from different datasets from 1996 to 2010

	NEIC	**RCMT**	**ETHZ**	**TDMT**
GCMT	0.10	0.07	0.08	0.14
NEIC		0.11	0.10	0.16
RCMT			0.09	0.12

Table 2 – Comparison between GCMT and RCMT catalogs from 2011 to 2018

Region	**N**	***α (intercept)***	***β (slope)***	**s.l. (H_0:β=1)**	**Δ *(mean difference)***	**s.l. (H_0:Δ=0)**
MED (all data)	308	0.345±0.051	0.939±0.010	**<0.01**	0.032±0.005	**<0.01**
ITA (all data)	44	0.283±0.117	0.951±0.023	**0.04**	0.030±0.010	**<0.01**
MED (Mw>5.4)	54	-0.016±0.157	1.001±0.027	0.97	-0.010±0.010	0.35
ITA (Mw>5.4)	10	0.172±0.325	0.971±0.056	0.62	0.004±0.014	0.77

Bold types indicate that the Student's t-test significantly rejects the H_0 hypothesis.

Table 3 – Comparison between GCMT and TDMT catalogs from 2011 to 2018

Region	**N**	***α (intercept)***	***β (slope)***	**s.l. (H_0:β=1)**	**Δ *(mean difference)***	**s.l. (H_0:Δ=0)**
MED (all data)	46	0.280±0.139	0.991±0.027	0.74	0.235±0.013	**<0.01**
ITA (all data)	34	0.298±0.120	0.983±0.024	0.49	0.214±0.011	**<0.01**
MED (Mw>5.4)	9	0.925±0.826	0.885±0.141	0.44	0.252±0.036	**<0.01**
ITA (Mw>5.4)	6	1.078±0.308	0.853±0.052	**<0.05**	0.214±0.026	**<0.01**

Bold types indicate that the Student's t-test significantly reject the H_0 hypothesis.

Table 4 – Comparison between GCMT and GFZP catalogs from 2011 to 2018

Region	N	α *(intercept)*	β *(slope)*	s.l. (H_0:β=1)	Δ *(mean difference)*	s.l. (H_0:Δ=0)
GBL (all data)	6704	0.226±0.009	0.971±0.002	**<0.01**	0.066±0.001	**<0.01**
MED (all data)	467	0.387±0.042	0.945±0.008	**<0.01**	0.105±0.004	**<0.01**
ITA (all data)	42	0.401±0.091	0.941±0.018	**<0.01**	0.098±0.010	**<0.01**
GBL (Mw>5.4)	3187	0.017±0.015	1.005±0.003	**0.03**	0.049±0.001	**<0.01**
MED(Mw>5.4)	87	-0.162±0.112	1.038±0.019	0.05	0.060±0.008	**<0.01**
ITA (Mw>5.4)	11	0.105±0.214	0.991±0.037	0.82	0.055±0.011	**<0.01**

Bold types indicate that the Student's t-test significantly reject the H_0 hypothesis.

Table 5 – Mean squared deviations σ_d between couples of corrected Mw taken from different datasets from 2011 to 2018

	RCMT	GFZP	TDMT
GCMT	0.07	0.06	0.09
RCMT		0.09	0.10
GFZP			0.12

Table 6 – Numbers of earthquakes (N) and Md estimated (N Md) reported by ISIDe before and after the migration to Earthworm acquisition software.

	16/4/2005 - 30/4/2012	%	1/5/2012 - 31/12/2018	%
N Total	83402		214013	
N Md	74116	88.9	16093	7.5
N Md<1.0	46	0.1	2817	17.5

Table 7 – Empirical standard deviations of regression residuals ($\sigma_{empirical}$), Mw average uncertainties ($\bar{\sigma}_{\mathrm{Mw}}$), and ML adjusted uncertainties **(**σ_{ML}) for different time intervals and datasets.

	$\boldsymbol{\sigma_{empirical}}$	$\boldsymbol{\bar{\sigma}_{\mathrm{Mw}}}$	$\boldsymbol{\sigma_{\mathrm{ML}}}$
*Gasperini et al. (2013a)**	*0.216*	*0.10*	*0.18*
2005-2010	0.207	0.10	0.17
2011-2018	0.182	0.07	0.16
2011-2018 no 6.6	0.181	0.07	0.16
2005-2018	0.189	0.08	0.16
2005-30/4/2012	0.207	0.09	0.17
1/5/2012-2018	0.180	0.07	0.16
2011-2012	0.216	0.07	0.21
2013-2014	0.190	0.07	0.17
2015-2016	0.181	0.07	0.15
2015-2016 no 6.6	0.179	0.07	0.15
2017-2018	0.136	0.07	0.11

*The first row reports the results obtained by Gasperini et al. (2013a) for 2005-2010.

Table 8 – Comparisons between Mw and ML in different time intervals.

Dataset	**N**				**Δ**	
		α (intercept)	**β (slope)**	**s.l. (H_0:β=1)**		**s.l. (H_0:Δ=0)**
*Gasperini et al. (2013a)**	*157*	*-0.164±0.127*	*1.066±0.031*	***0.03***	*0.103±0.016*	***<0.01***
2005-2010	187	-0.157±0.120	1.066±0.029	**0.02**	0.113±0.015	**<0.01**
2011-2018	495	-0.056±0.064	1.042±0.016	**<0.01**	0.109±0.008	**<0.01**
2011-2018 no 6.6	494	-0.030±0.065	1.035±0.016	**0.03**	0.108±0.008	**<0.01**
2005-2018	682	-0.078±0.056	1.047±0.014	**<0.01**	0.110±0.007	**<0.01**
2005-30/4/2012	228	-0.089±0.109	1.051±0.027	0.06	0.117±0.013	**<0.01**
1/5/2012-2018	454	-0.079±0.066	1.047±0.017	**<0.01**	0.106±0.008	**<0.01**
2011-2012	90	0.163±0.174	0.976±0.041	0.57	0.064±0.023	**<0.01**
2013-2014	114	-0.105±0.152	1.058±0.039	0.14	0.119±0.017	**<0.01**
2015-2016	170	-0.256±0.108	1.097±0.027	**<0.01**	0.125±0.013	**<0.01**
2015-2016 no 6.6	169	-0.212±0.113	1.085±0.029	**<0.01**	0.122±0.013	**<0.01**
2017-2018	121	-0.039±0.105	1.039±0.028	0.15	0.111±0.012	**<0.01**

Bold types indicate that the Student's t-test significantly reject the relevant H_0 hypothesis of equality. *The first row reports the results obtained by Gasperini et al. (2013a) for years 2005-2010.

Table 9 – Coefficients of magnitude conversion applied to various datasets

Dataset	**Time interval**	**Mtype**	**α (intercept)**	**β (slope)**	**Cov(a,b)**
GCMT	-	Mw	0.00	1.00	-
RCMT	-	Mw	0.00	1.00	-
NEIC	-	Mw	+0.05	1.00	-
ETHZ	-	Mw	-0.05	1.00	-
GFZP	-	Mw	+0.05	1.00	-
TDMT	-	Mw	+0.20	1.00	-
ISIDe	<2011	ML	-0.164±0.127	1.066±0.031	-0.0038
ISIDe	≥2011	ML	-0.030±0.065	1.035±0.016	-0.0011
ISIDe	< 01/04/2013	Md	-1.905±0.205	1.718±0.050	-0.0063
ISIDe	≥ 01/04/2013	Md	-1.132±0.205*	1.718±0.050	-0.0063

* The Md intercept includes the empirical correction of +0.45 to Md since 01/04/2013

748

749 Table 10 – Completeness thresholds of HORUS catalog as a function of time according to

750 Gasperini et al. (2013a) (1981-2010) and Lolli et al. (2018) (1960-1980),

Time interval	***Mc***	***b*-value**
1960-1980	4.0	1.02±0.03
1981-1989	3.0	0.97±0.02
1990-1996	2.5	0.95±0.02
1997-2002	2.5	0.94±0.01
2003-15/04/2005	2.1	1.01±0.03
16/04/2005-2010	1.8	0.97±0.01

751

752

753

754

Figure captions

Figure 1 – Regression between Mw from GCMT and GFZP global catalogs, using all data (a) and using only those with Mw GFZP >5.4 (b).

Figure 2 – Distribution of Md-ML pairs from ISIDe, before (circles) and after (crosses) 1 Apr 2013.

Figure 3 – Average differences between ML and Md (dotted), between Mw proxies computed from ML and Md (solid) and between Mw proxies computed from ML and from Md + 0.45 (dashed), in different time intervals.

Figure 4 – Regressions between Mw from IMT and ML from ISIDe from 2011 to 2018 but excluding the shock of 30 October 2016 at 6:40 UTC with Mw=6.6 (ML=6.1).

Figure 5 – Cumulative (solid line) and non-cumulative (black circles) frequency magnitude distribution of Mw (true and proxies) from 01/05/2012 to 2019 not using (a) and using (b) the randomization of the second decimal of ML from ISIDe (see text).

Figure 6 – Same as Fig. 4 from 16 April 2005 to 30 April 2012.

Figure 7 – Cumulative (solid line) and non-cumulative (black circles) frequency-magnitude distribution of HORUS catalog (a) and of ISIDe online dataset (b). Thin solid lines indicate the GR law computed for data with magnitude not lower than the completeness threshold Mc=1.8. Upper right insets display the ratio between observed and predicted numbers of data with magnitude ≥Mmin. Lower left insets display *b*-value as a function of cut-off magnitude Mmin. The vertical dashed lines indicate the estimated completeness magnitude threshold (1.8).

Figure 8 – a) completeness magnitude Mc in various years computed by the interactive method (dark grey solid line) and by the corrected maximum curvature method (light grey solid line). Dashed lines display Mc for the entire catalog from 2005 to 2019. Thin solid lines indicate the Mc linear trend from 2005 to 2019. Black lines display the decimal logarithm of the observed (solid) and computed (dashed) numbers of earthquakes with Mw≥2.5 in each year. b) *b*-value in various years computed using Mc by the interactive method (dark grey solid line) and by the corrected maximum curvature method (light grey solid line). Dashed lines display the *b*-value for the entire catalog from 2005 to 2019.

Figure 9 – Completeness magnitude Mc computed by the interactive method (dark grey solid line) and by the corrected maximum curvature method (light grey solid line), in the months from September 2008 to April 2010. Dashed lines display Mc for year 2009. Thin solid lines indicate the Mc linear trend in year 2009. Black lines display the decimal logarithm of the observed (solid) and computed (dashed) annual rates of earthquakes with Mw≥2.5 in each month.

Figure 10 – Same as Fig. 9 from September 2011 to April 2013. Dashed and thin solid lines display Mc for year 2012 and the Mc linear trend in year 2012 respectively.

Figure 11 – Same as Fig. 9 from September 2015 to April 2017. Dashed and thin solid lines display Mc for year 2016 and the average Mc trend in year 2016 respectively.

Figure 1

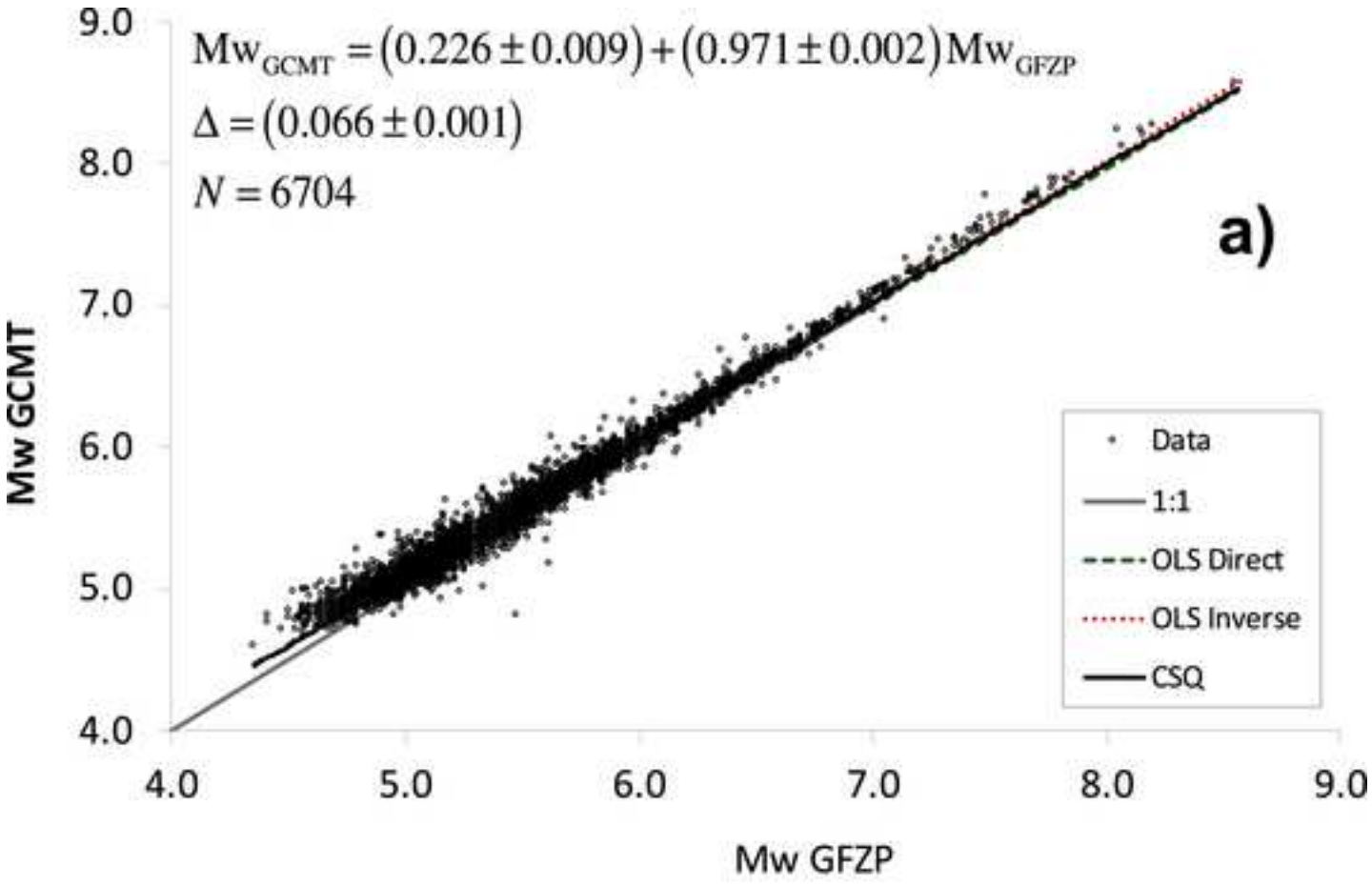

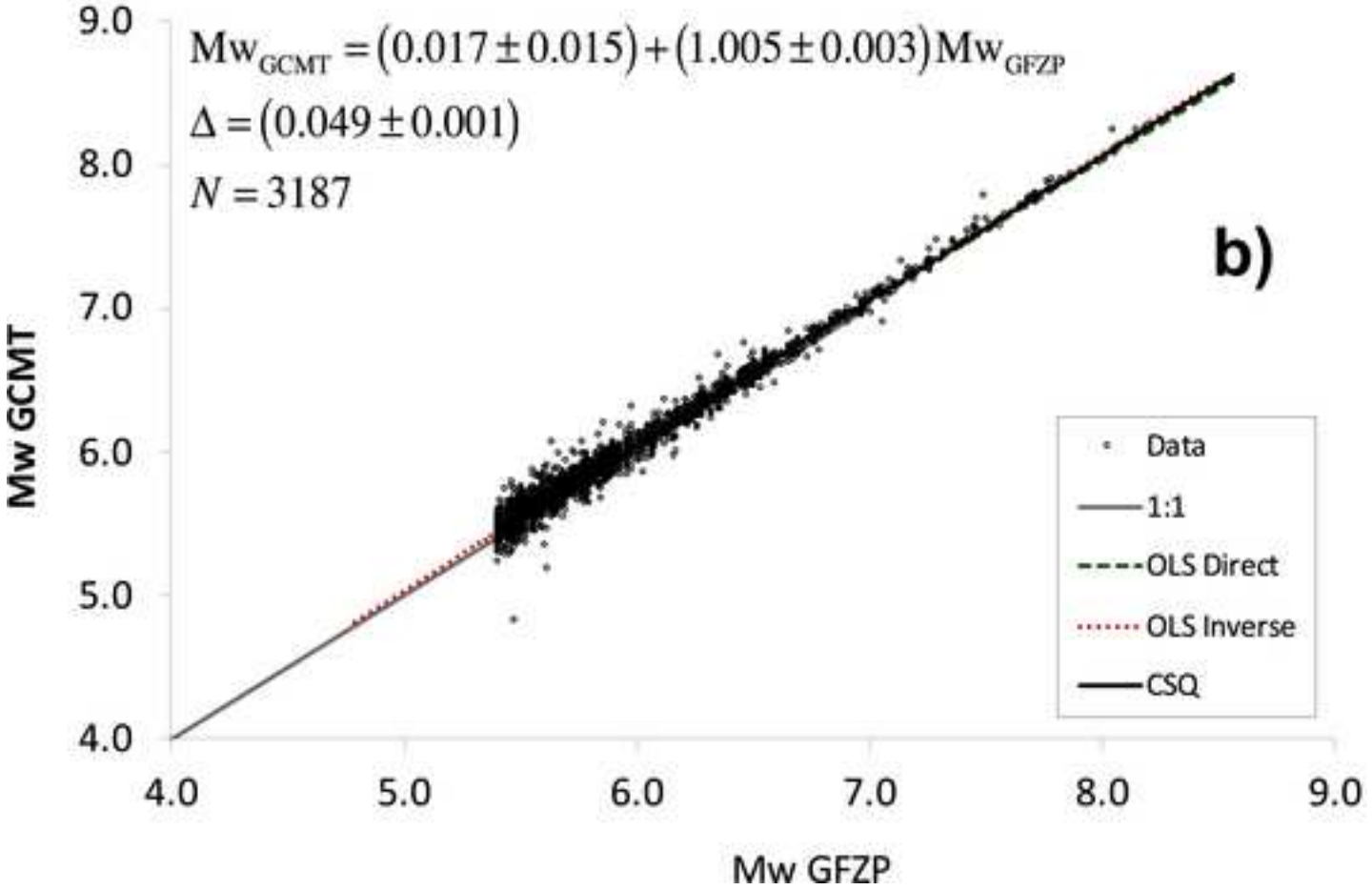

Figure 2

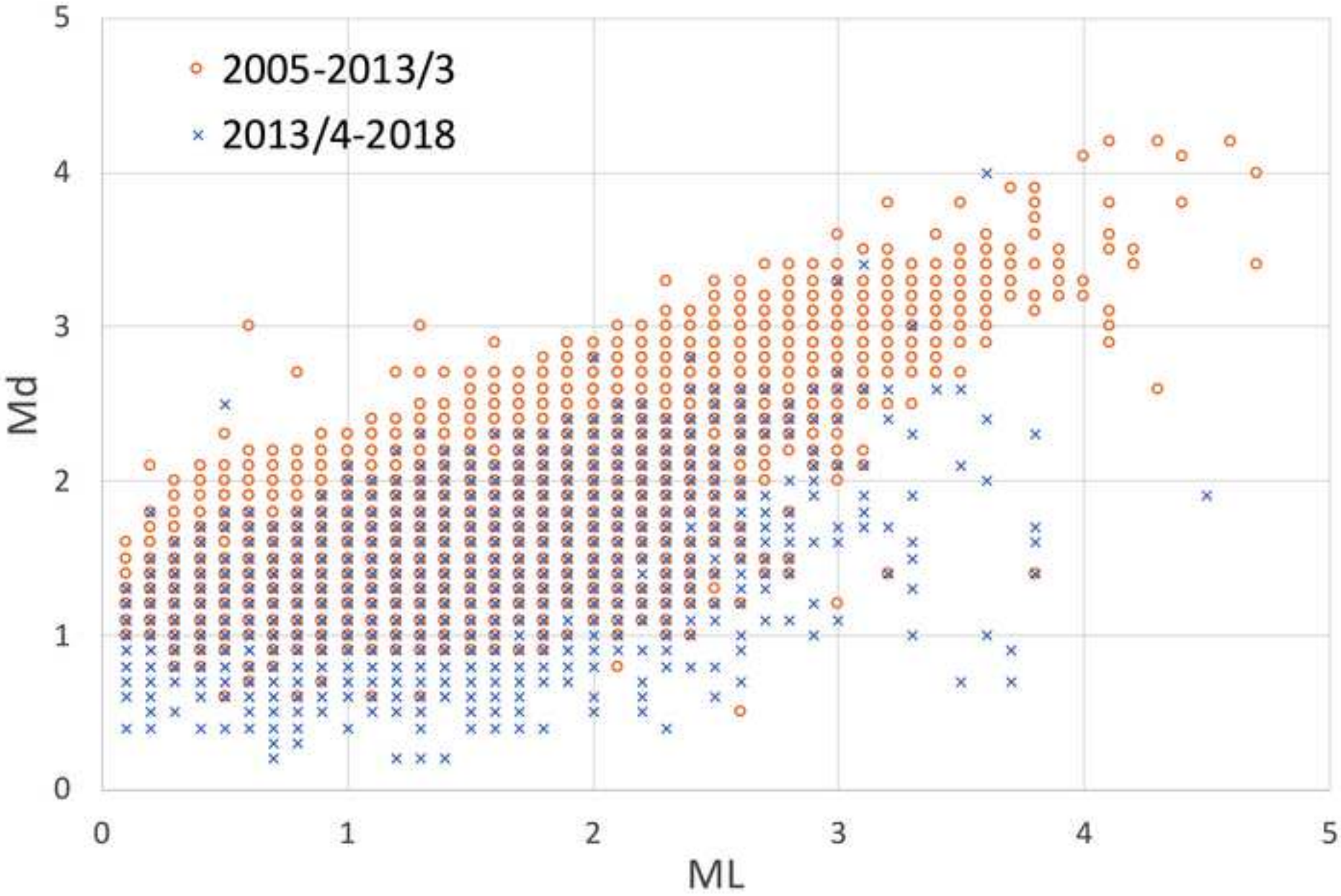

Figure 3

Click here to access/download;Figure;Fig_03.tif

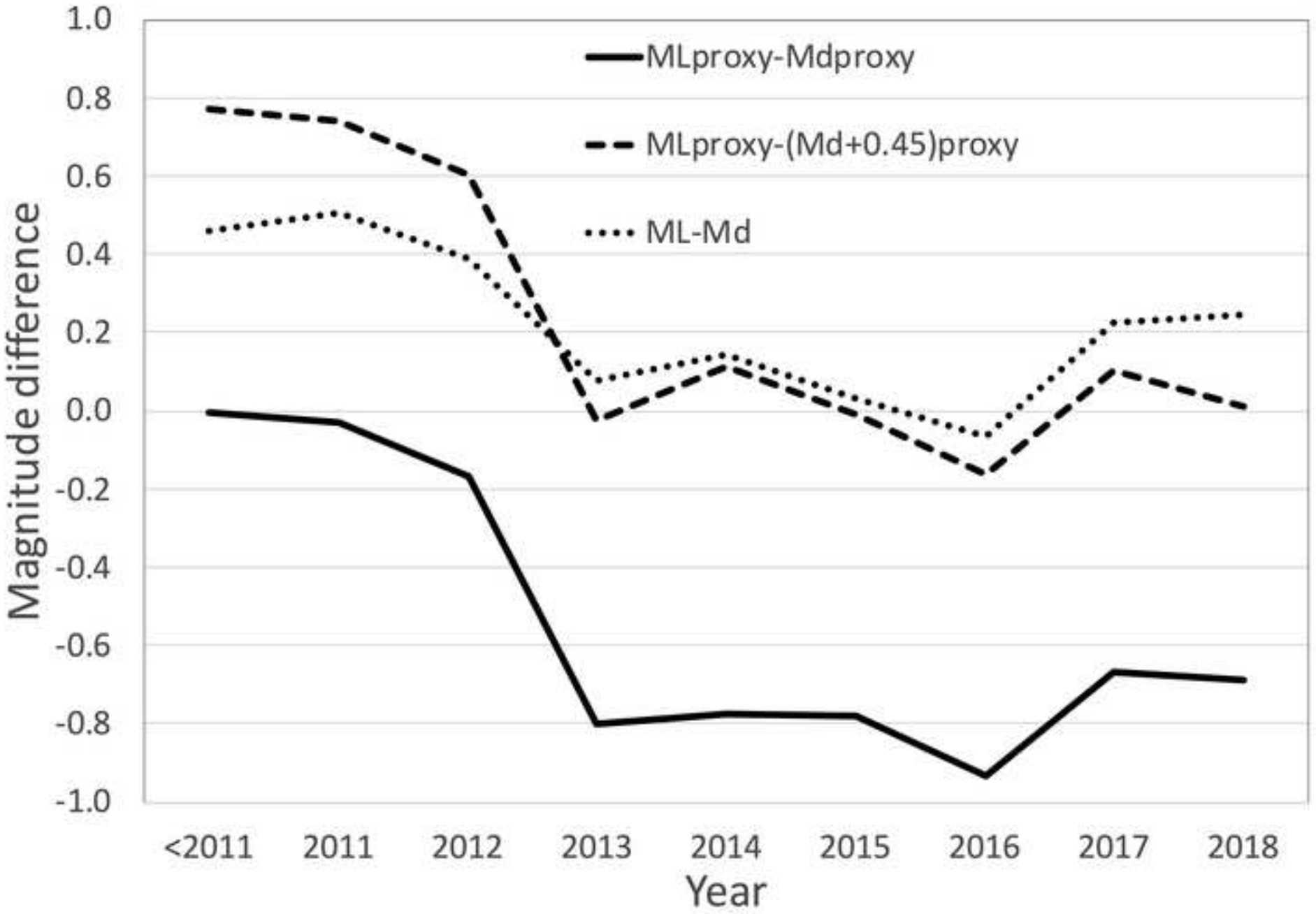

Figure 4

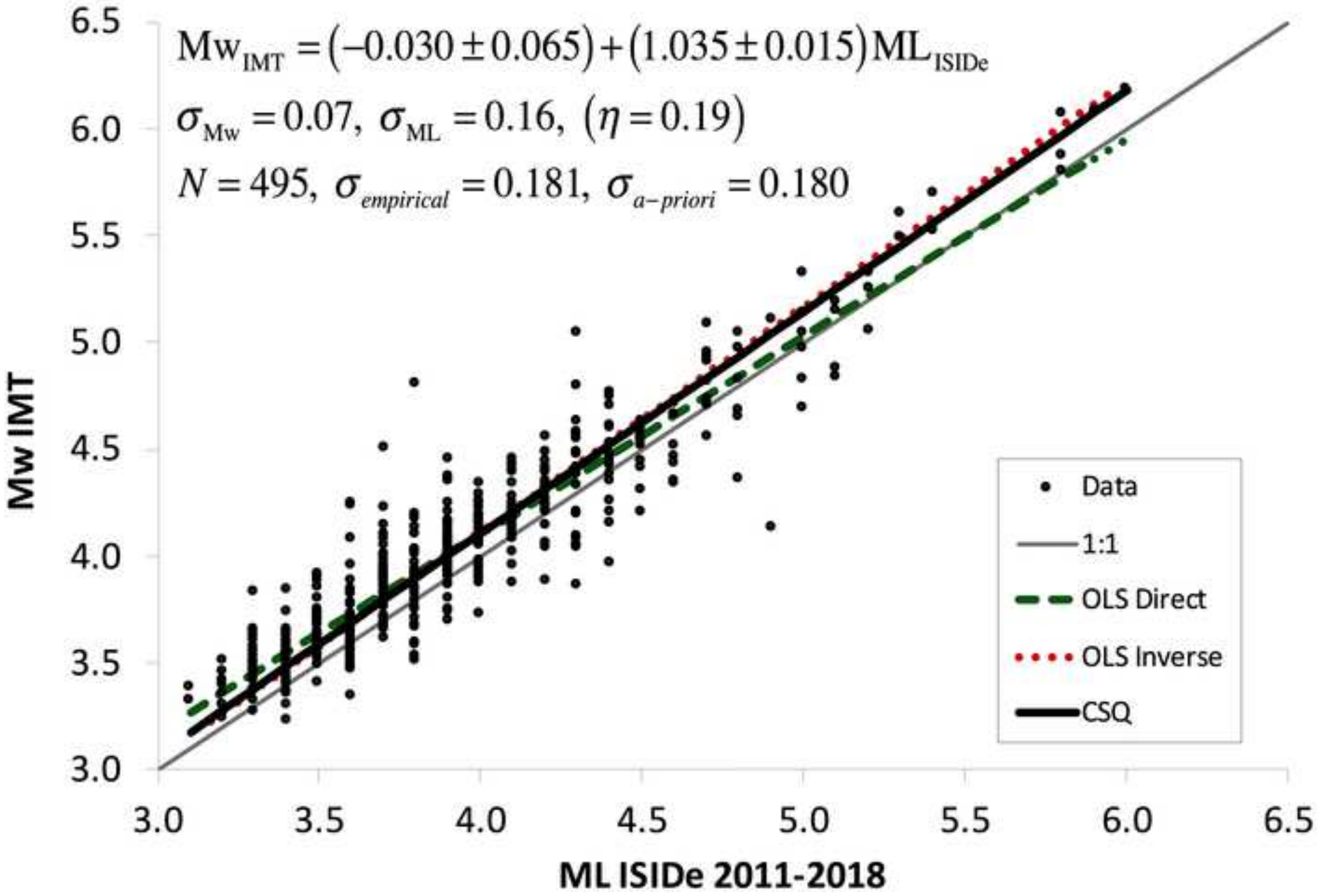

Figure 5

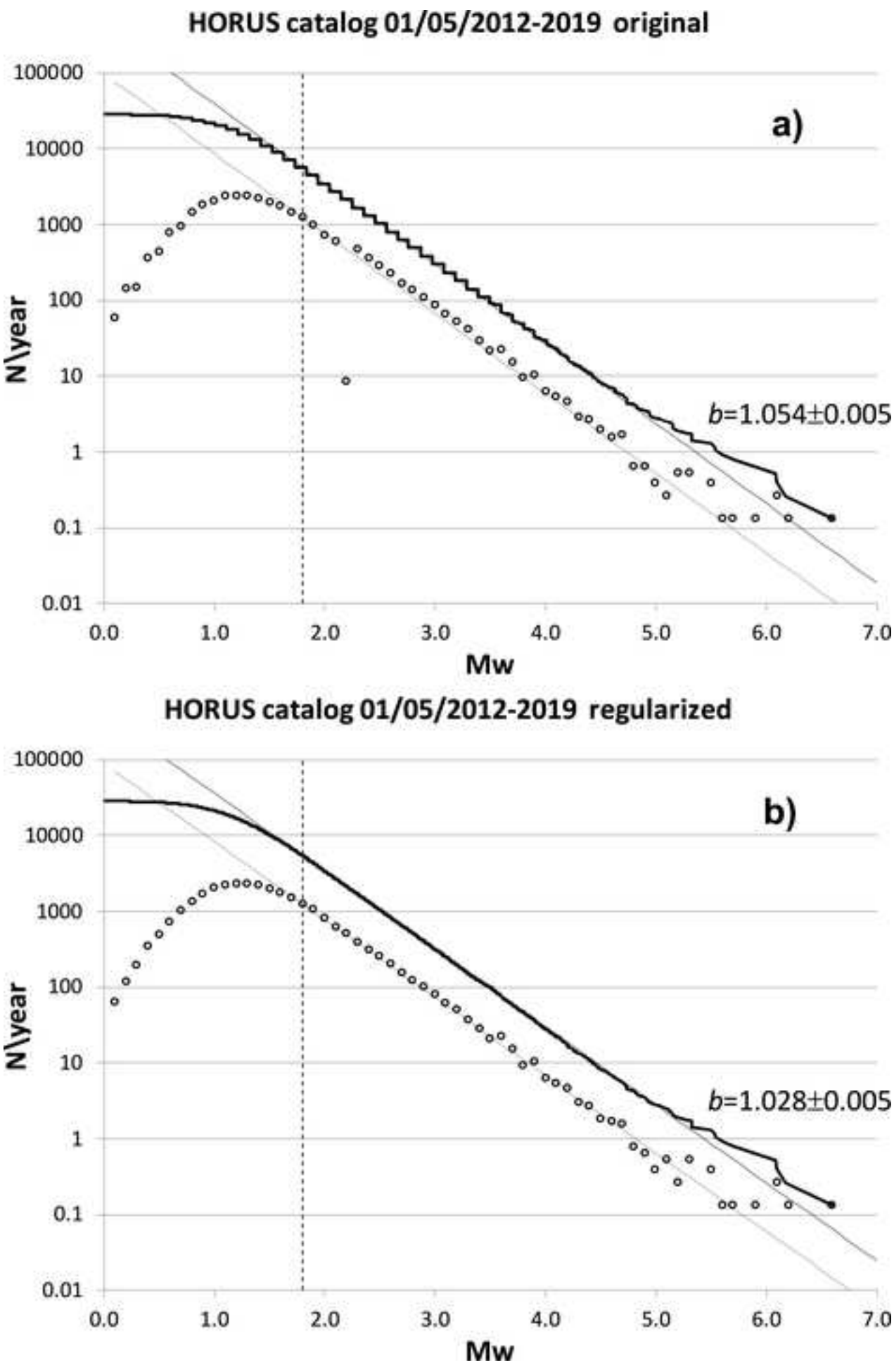

Figure 6

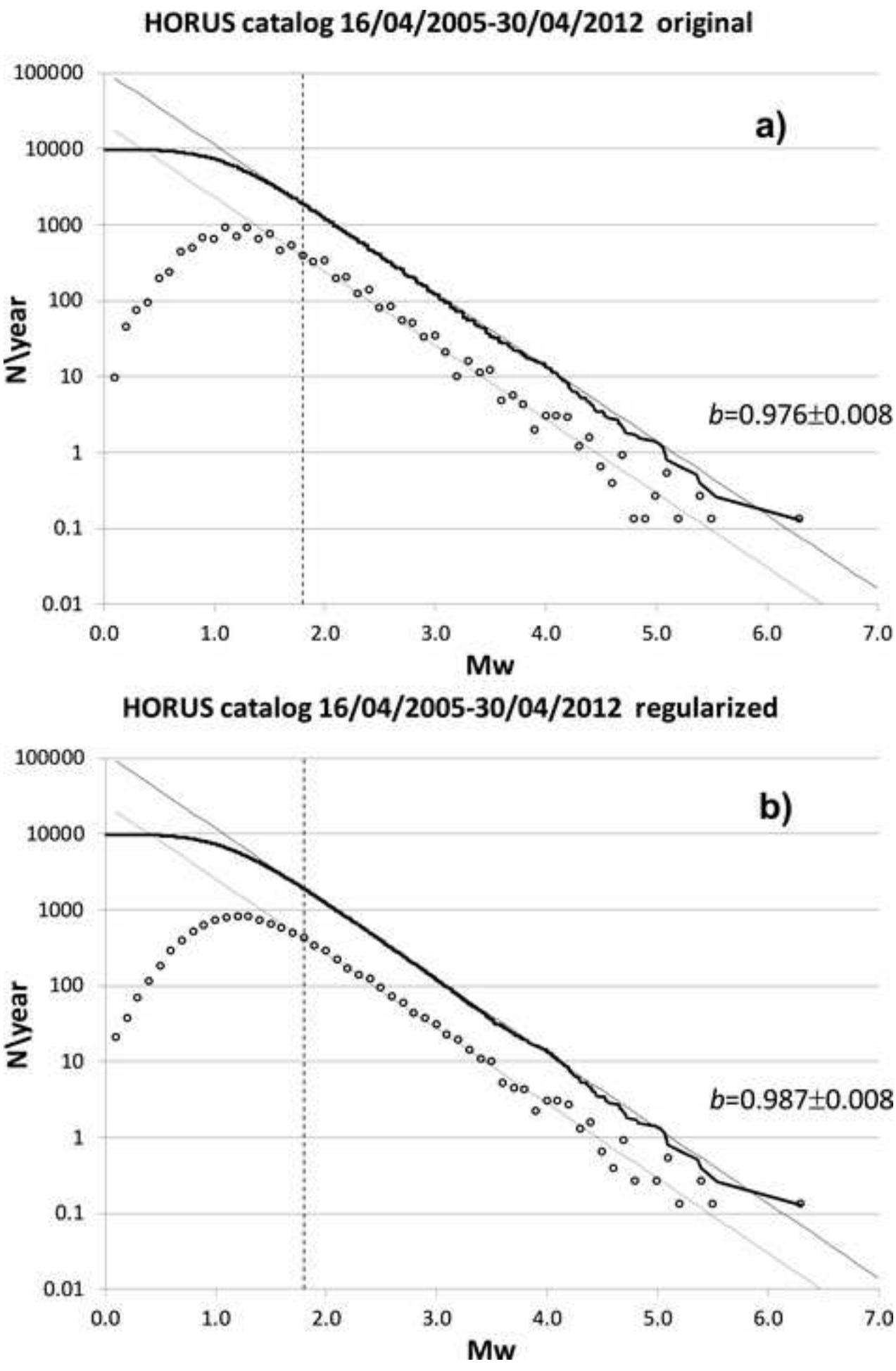

Figure 7

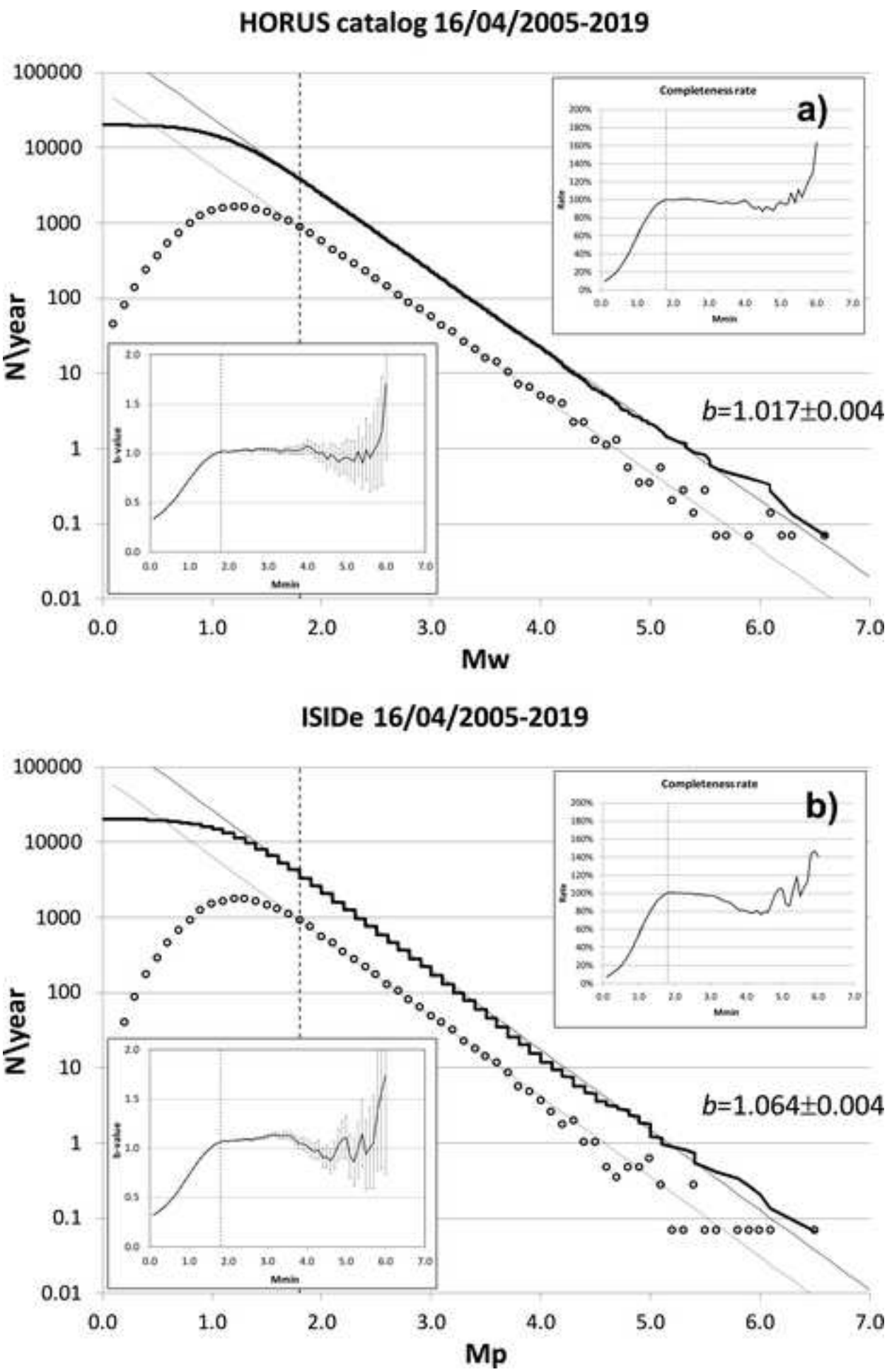

Figure 8

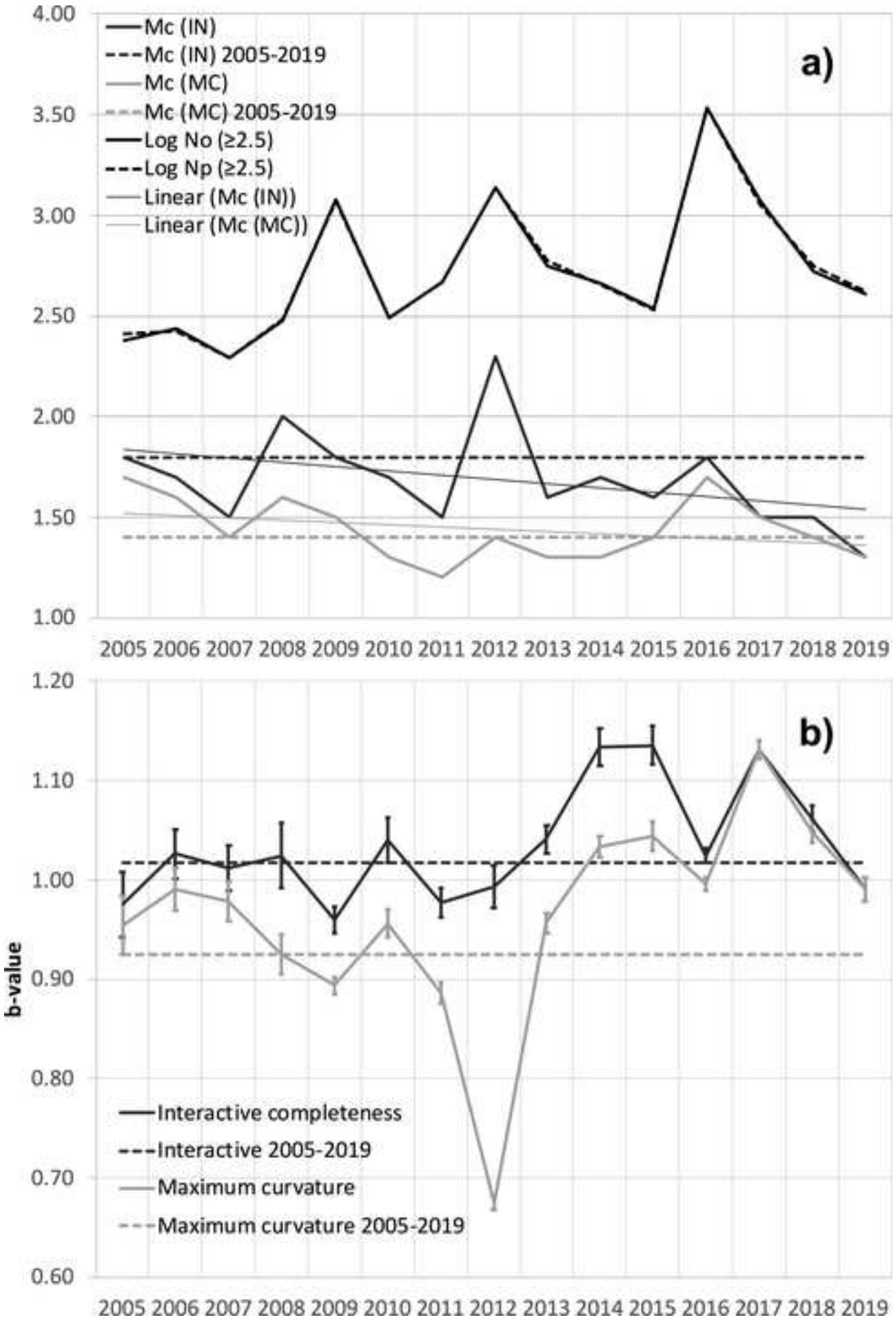

Figure 9

Click here to access/download;Figure;Fig_09.tif

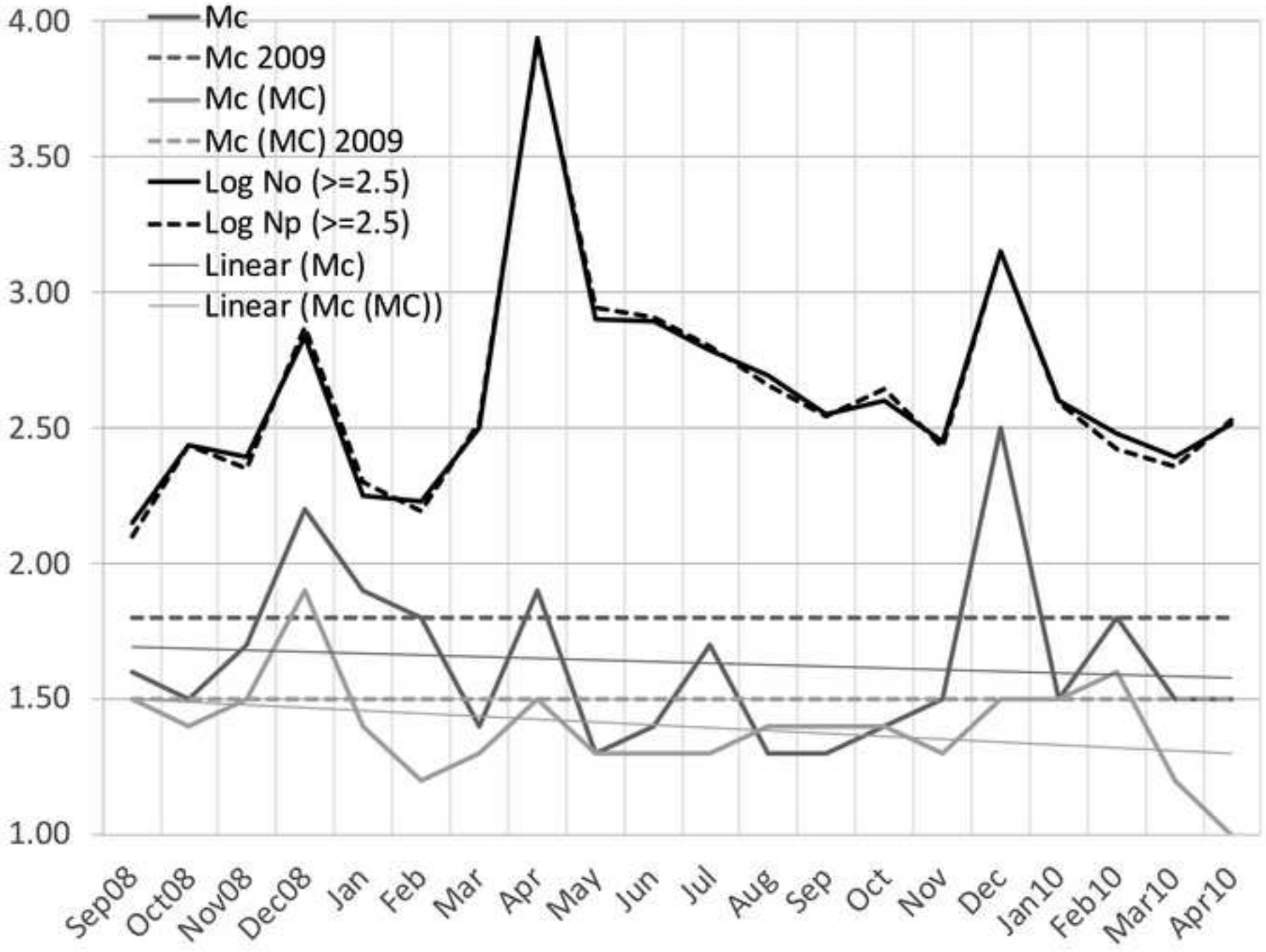

Figure 10

Click here to access/download;Figure;Fig_10.tif

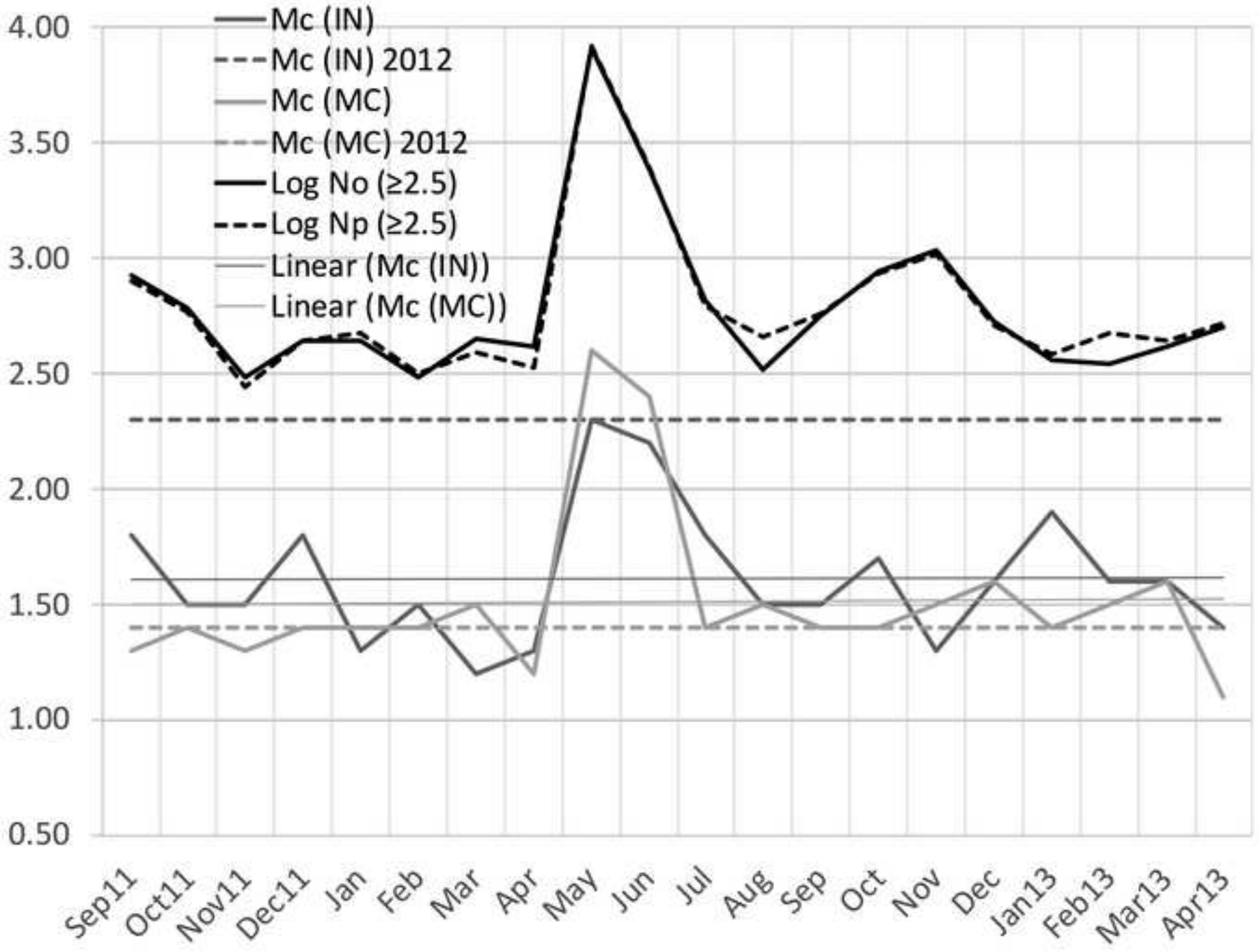

Figure 11

Click here to access/download;Figure;Fig_11.tif

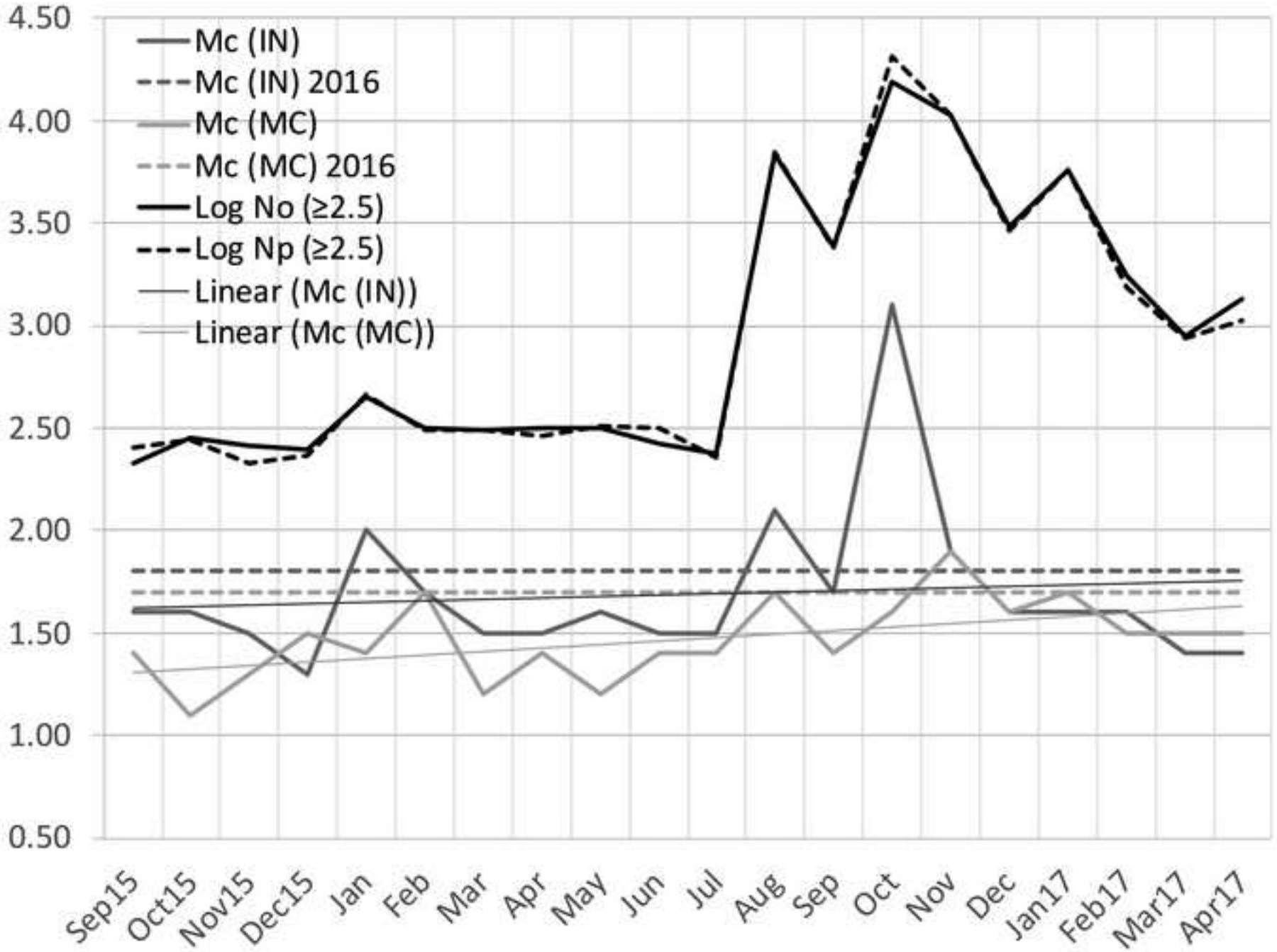

The HOmogenized instRUmental Seismic catalog (HORUS) of Italy from 1960 to present

Barbara Lolli[1]*, Daniele Randazzo[1], Gianfranco Vannucci[1] and Paolo Gasperini[2,1]

[1]Istituto Nazionale di Geofisica e Vulcanologia, Sezione di Bologna
[2]Dipartimento di Fisica e Astronomia, Università di Bologna

***Corresponding author: barbara.lolli@ingv.it**

Supplemental material

Supplemental material includes additional figures (from S1 to S15) and tables (from S1 to S5) useful to better describe methods and results.

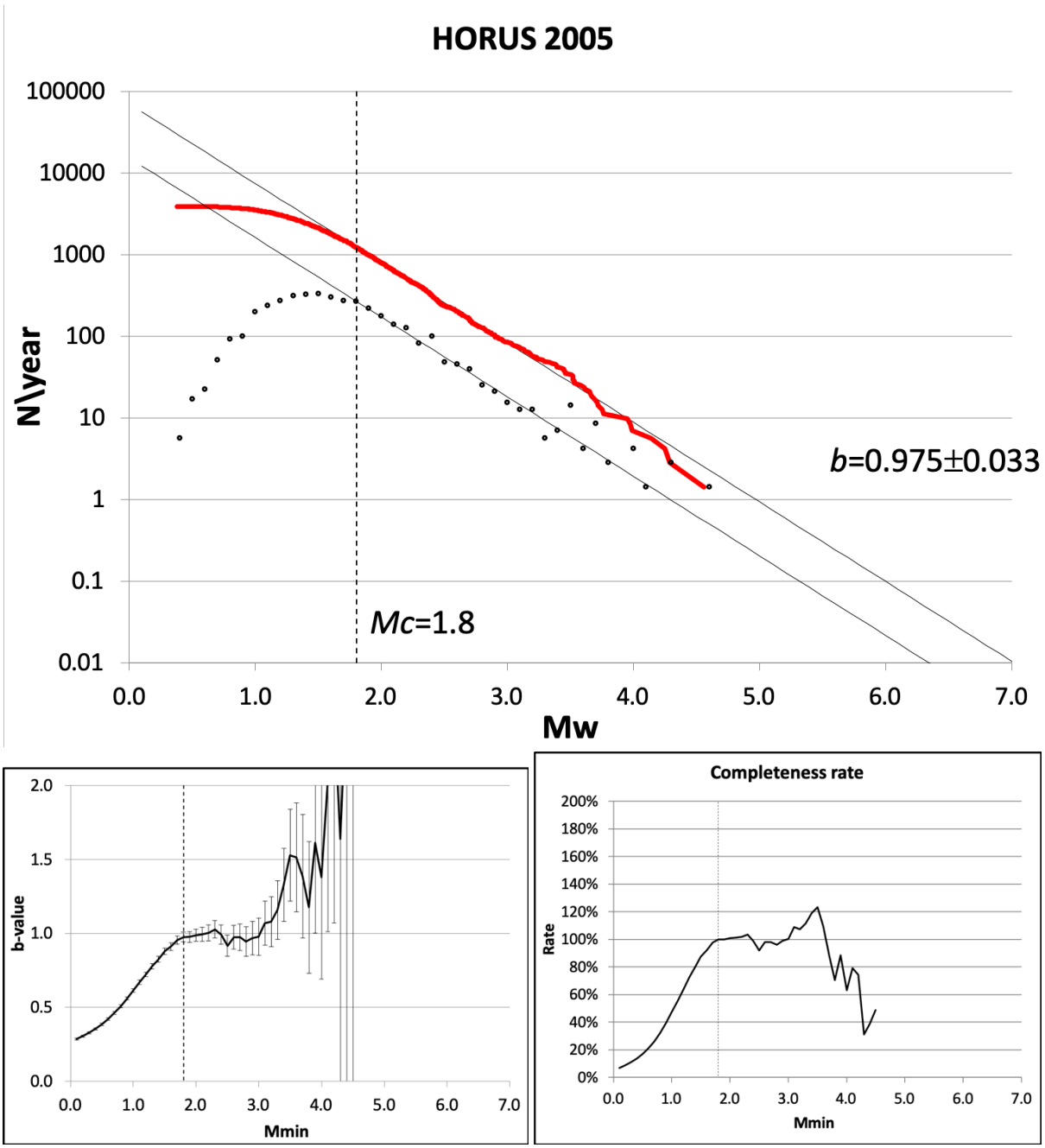

Figure S1 – Top: cumulative (red solid line) and non-cumulative (black circles) frequency-magnitude distribution of HORUS catalog for year 2005. The thin solid lines indicate the GR law computed for data with Mw not lower than the completeness threshold Mc. Bottom left: *b*-value as a function of cut-off magnitude Mmin. Bottom right: ratio between observed numbers of data with Mw≥Mmin and those predicted by the GR law. The vertical dashed lines indicate the estimated completeness magnitude threshold Mc.

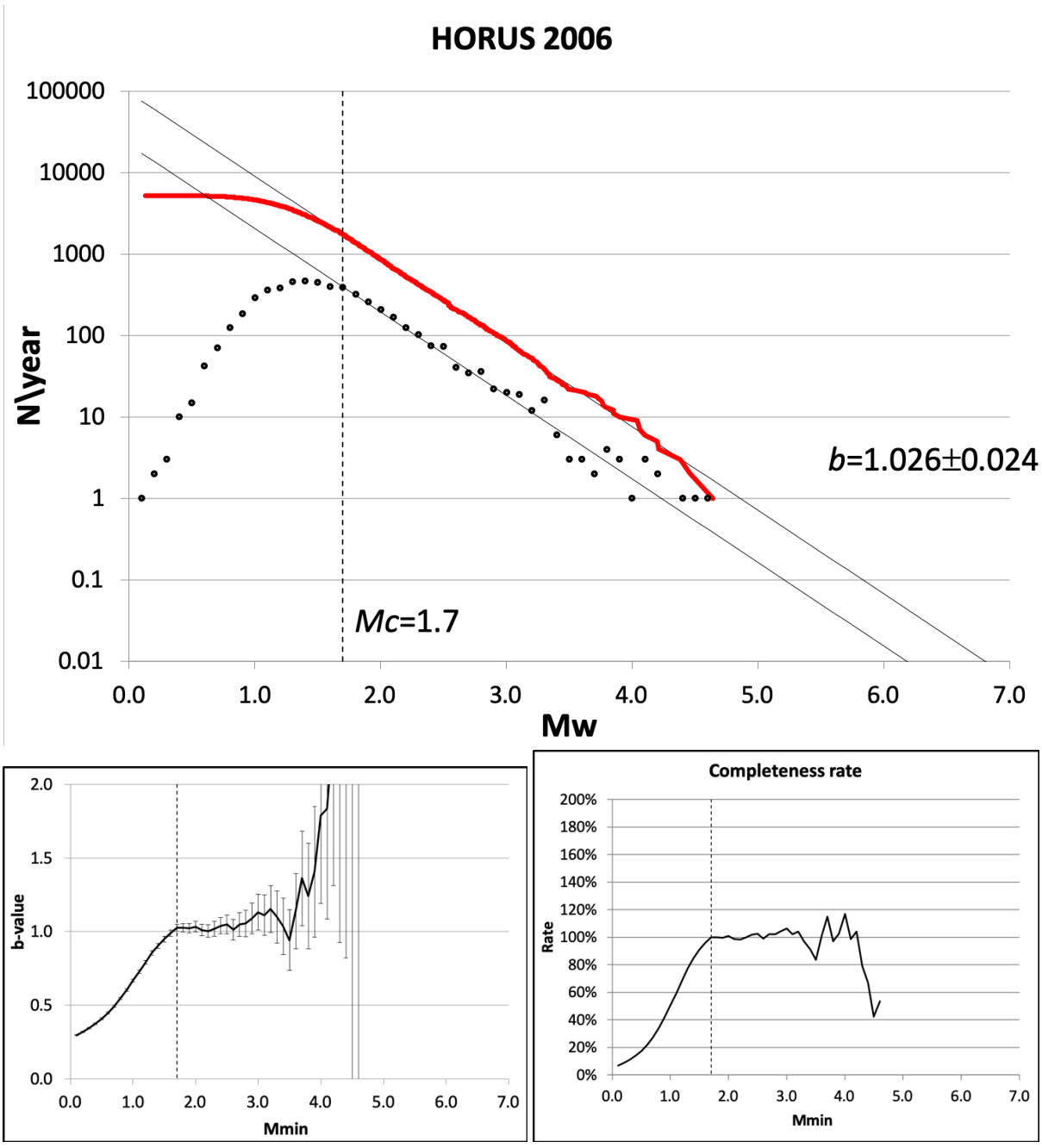

Figure S2 – Same as Fig. S1 for year 2006.

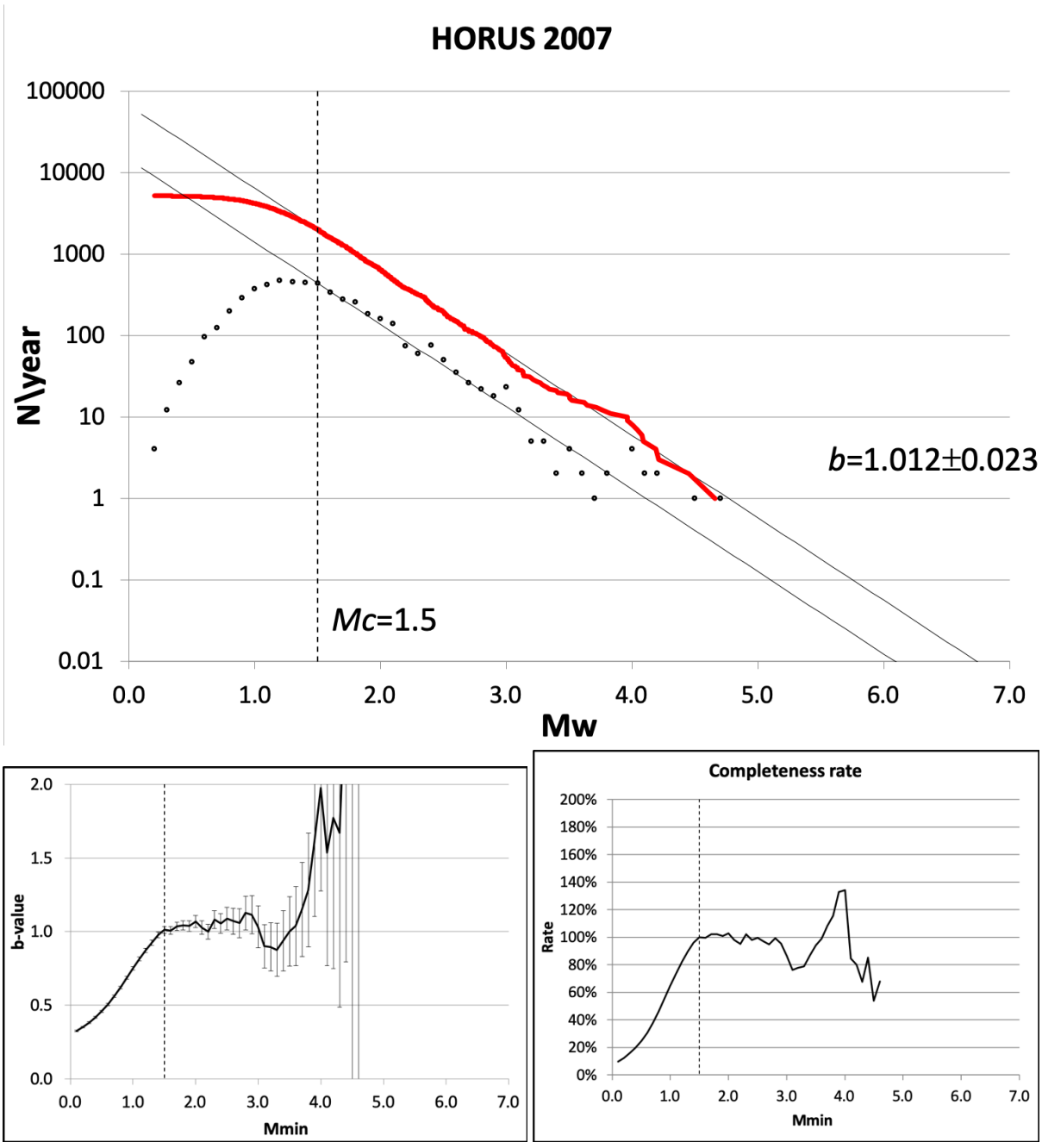

Figure S3 – Same as Fig. S1 for year 2007.

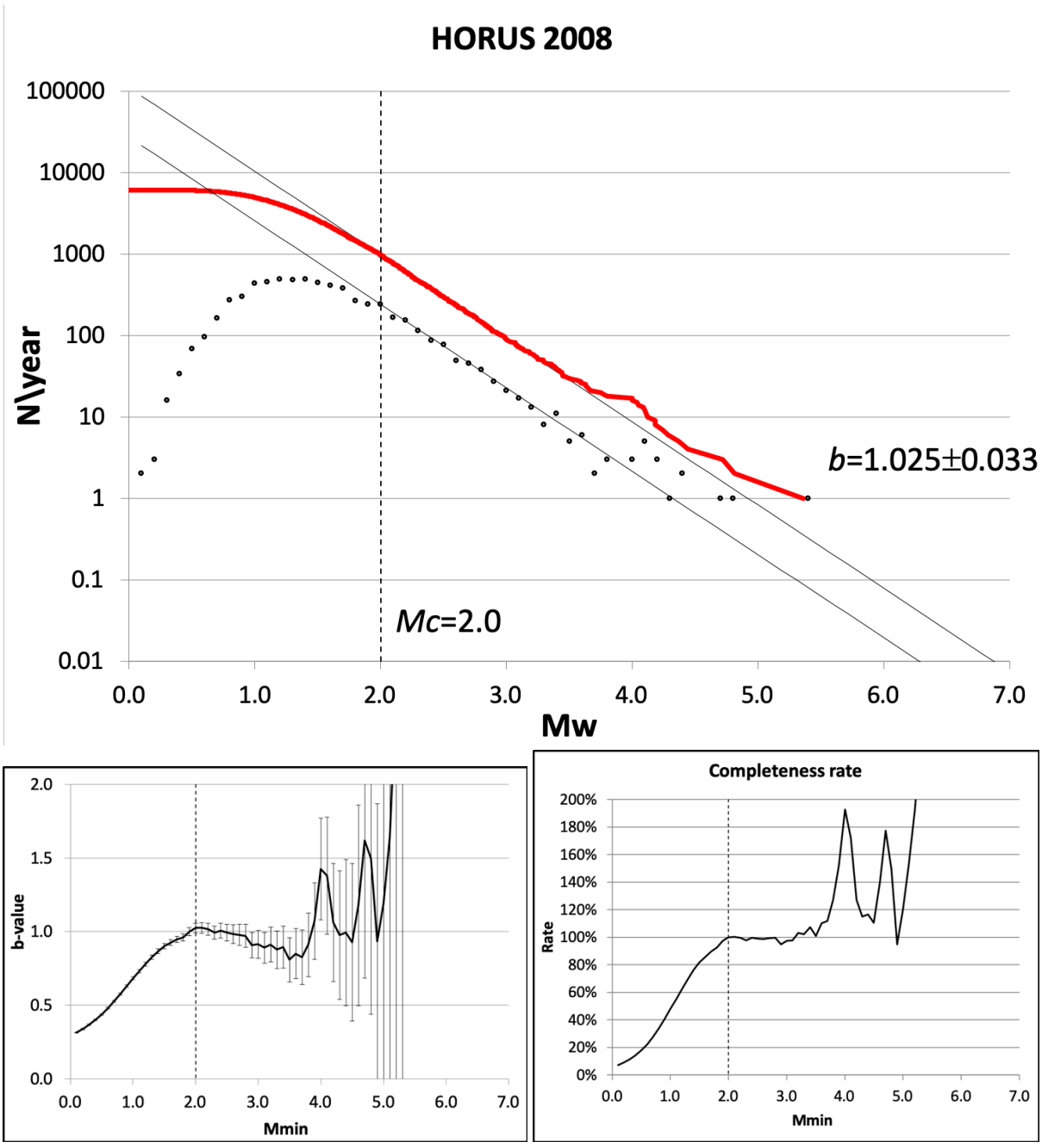

Figure S4 – Same as Fig. S1 for year 2008.

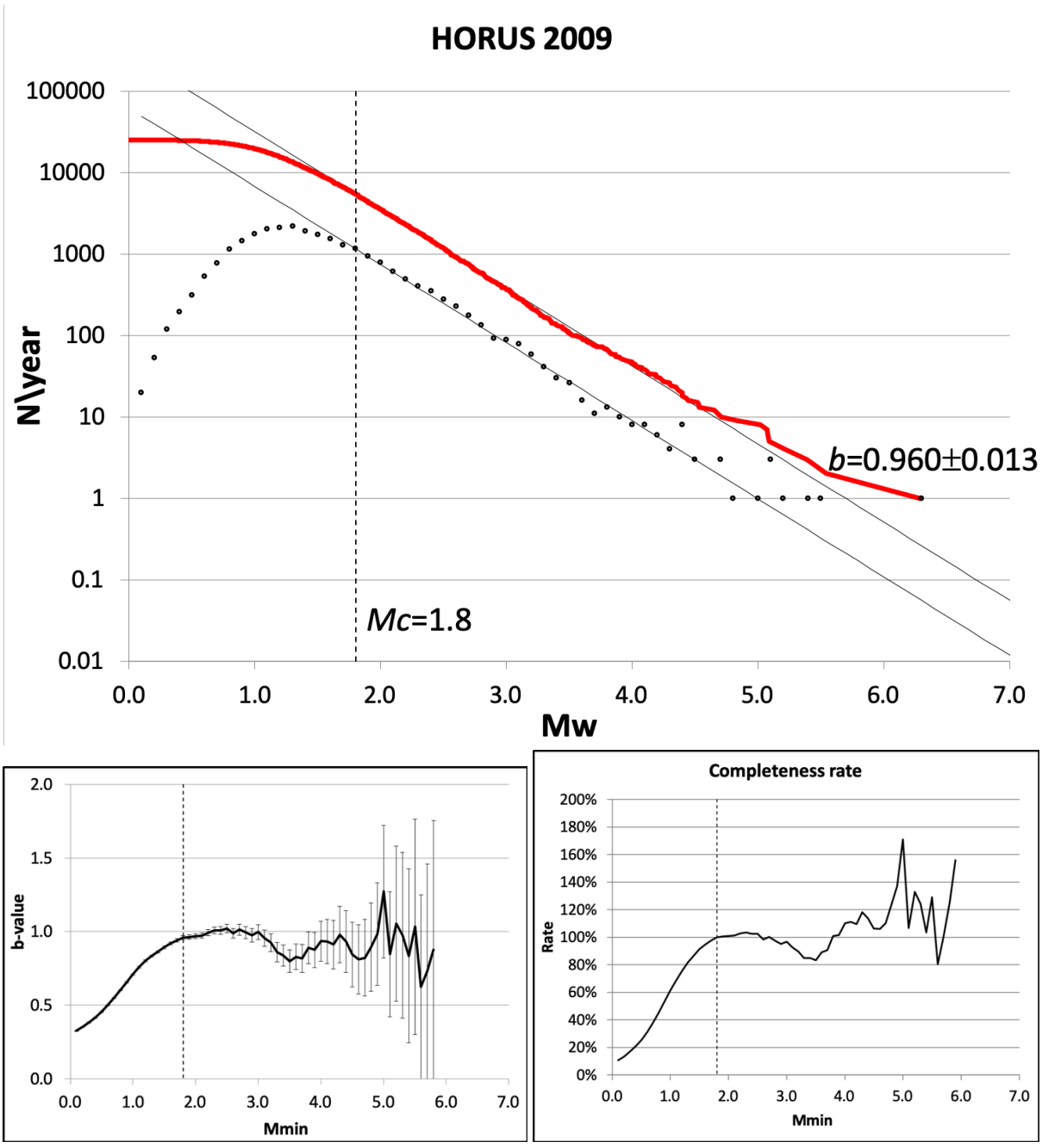

Figure S5 – Same as Fig. S1 for year 2009.

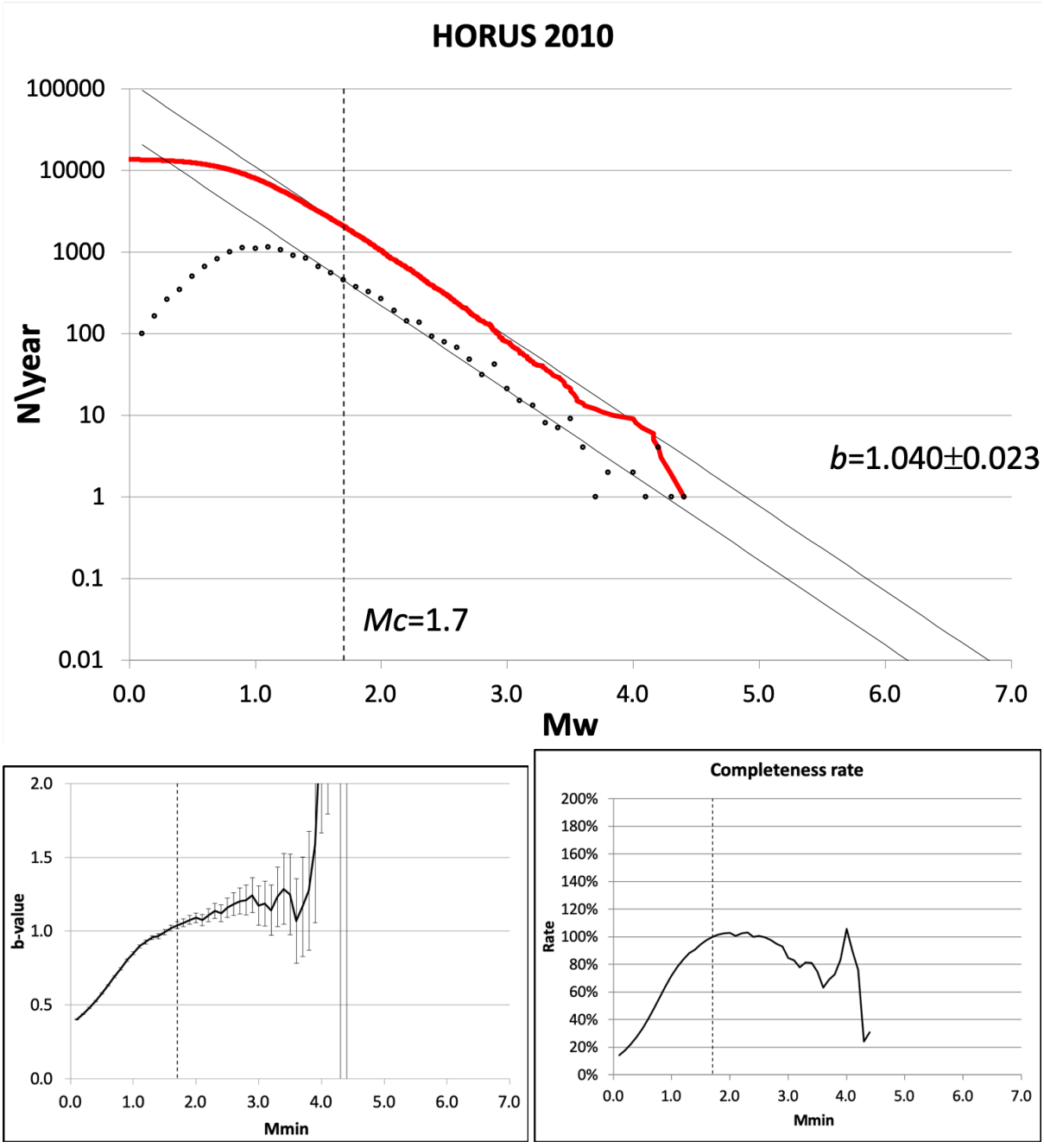

Figure S6 – Same as Fig. S1 for year 2010.

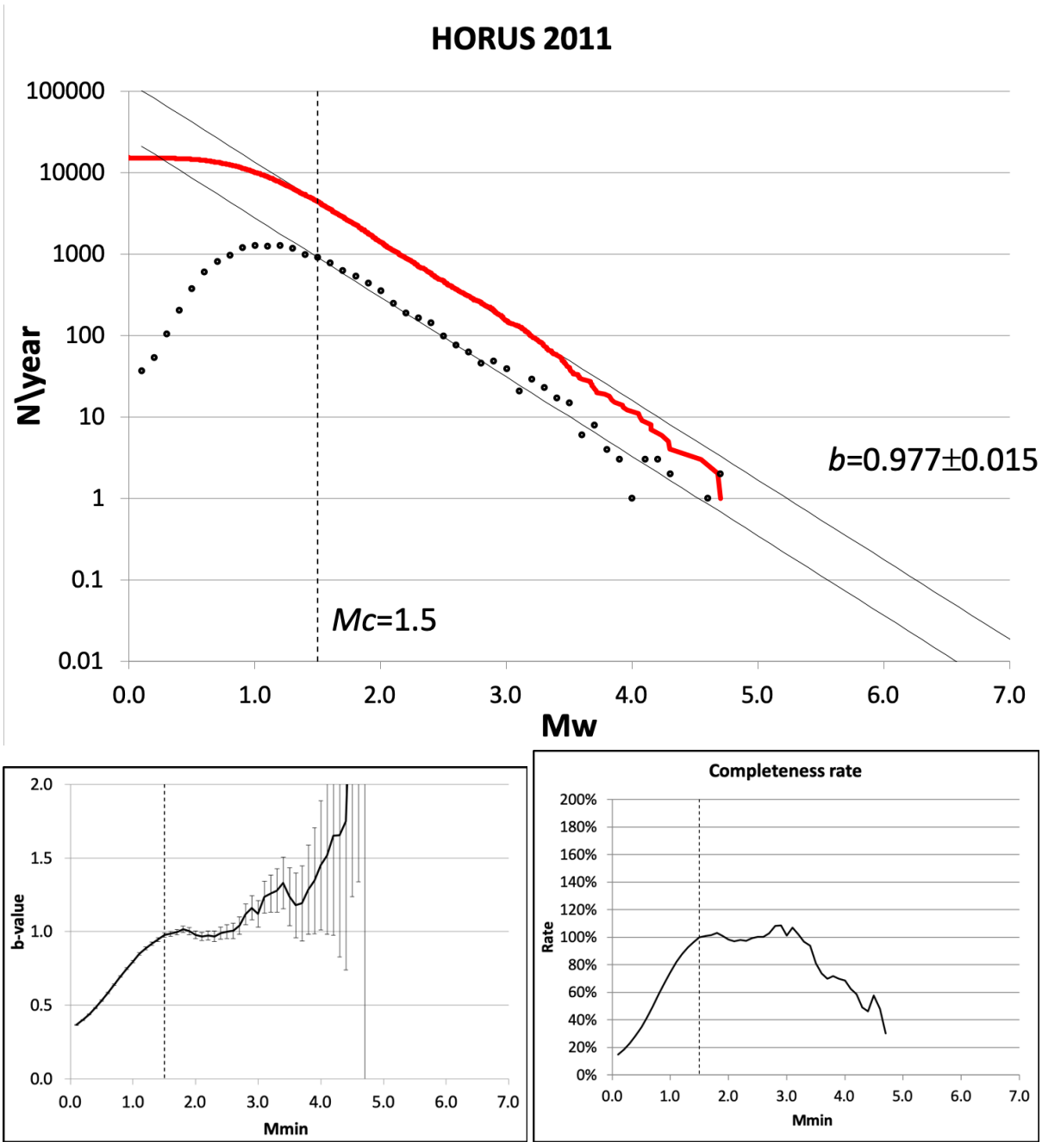

Figure S7 – Same as Fig. S1 for year 2011.

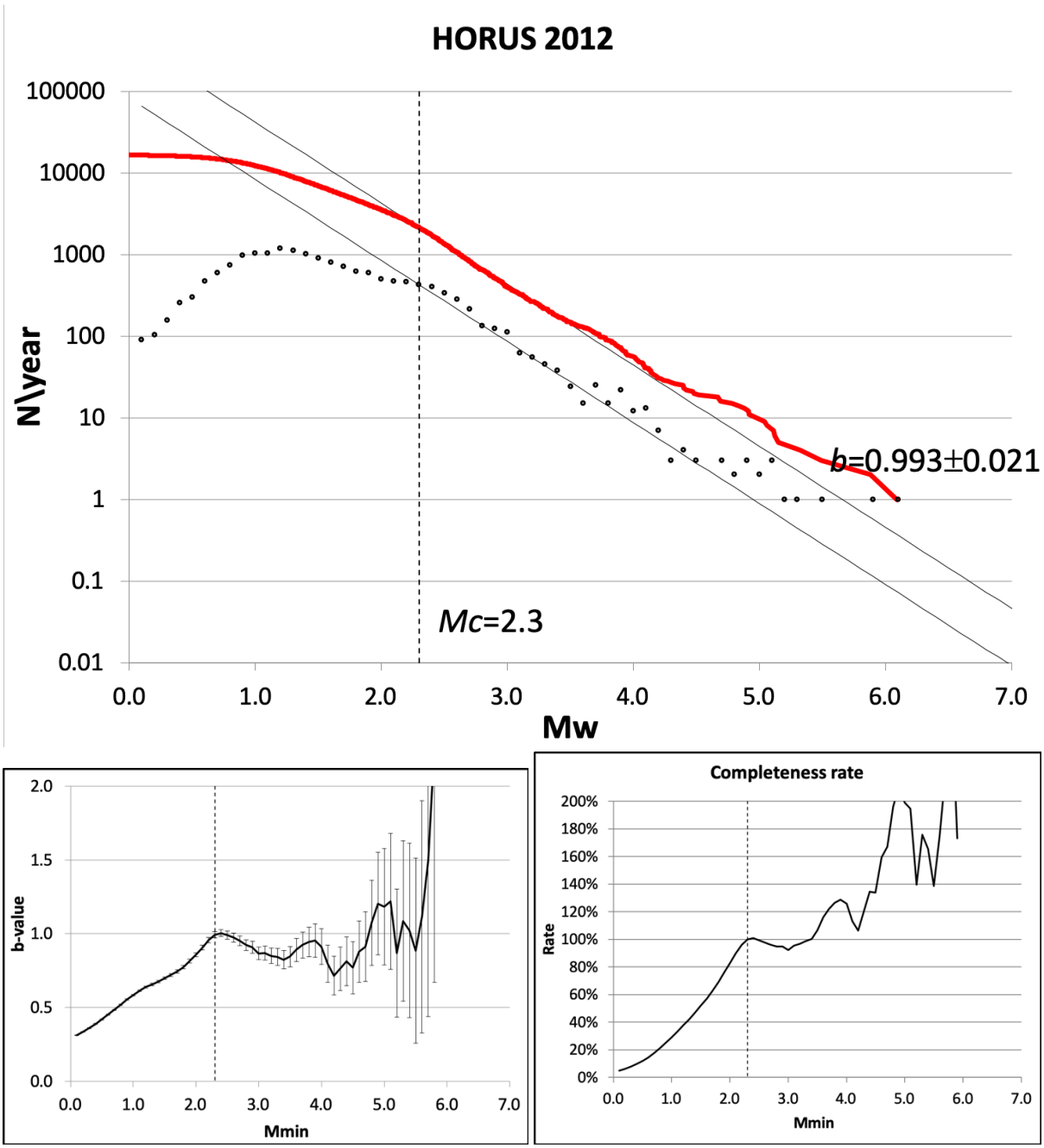

Figure S8 – Same as Fig. S1 for year 2012.

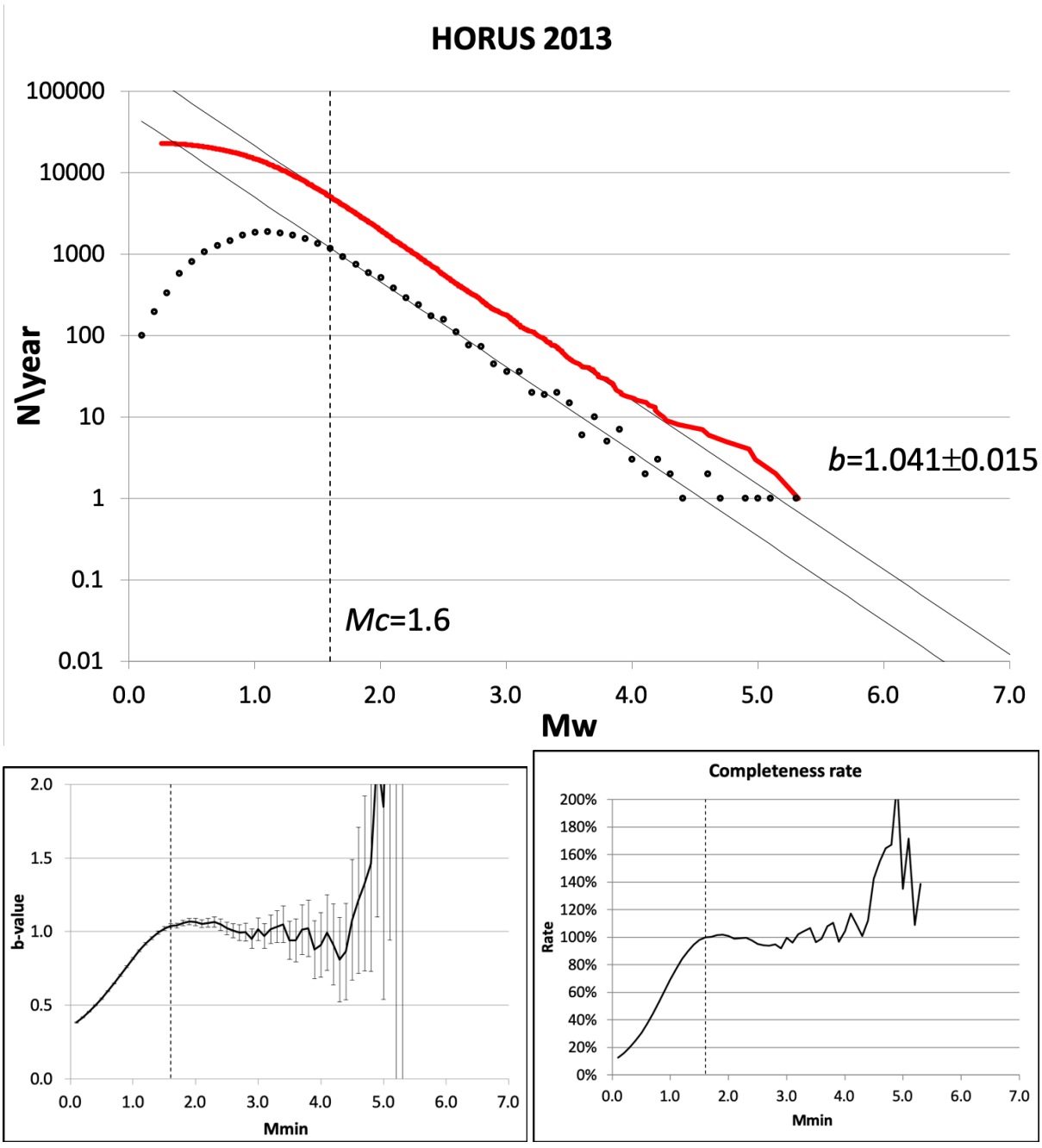

Figure S9 – Same as Fig. S1 for year 2013.

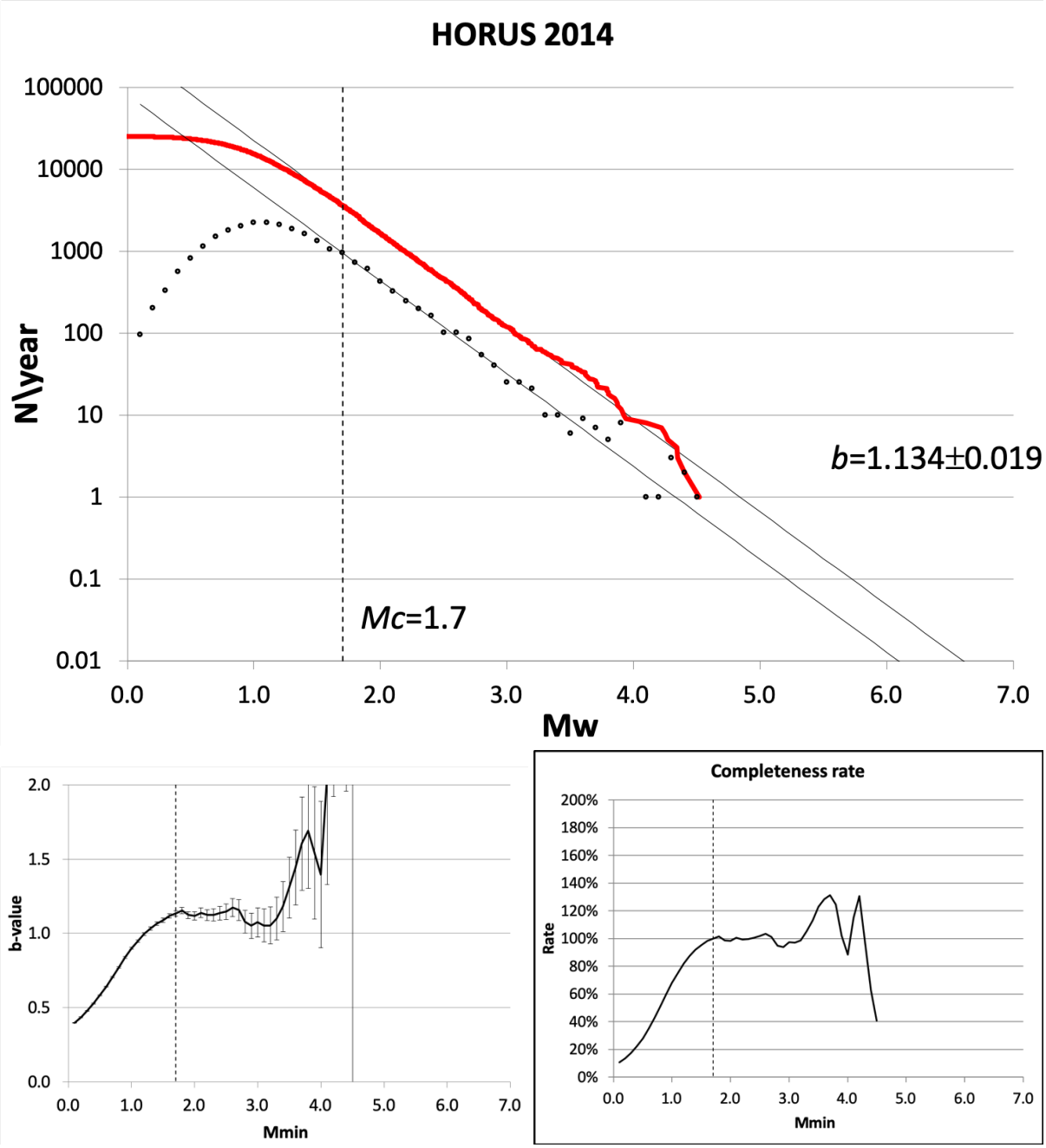

Figure S10 – Same as Fig. S1 for year 2014.

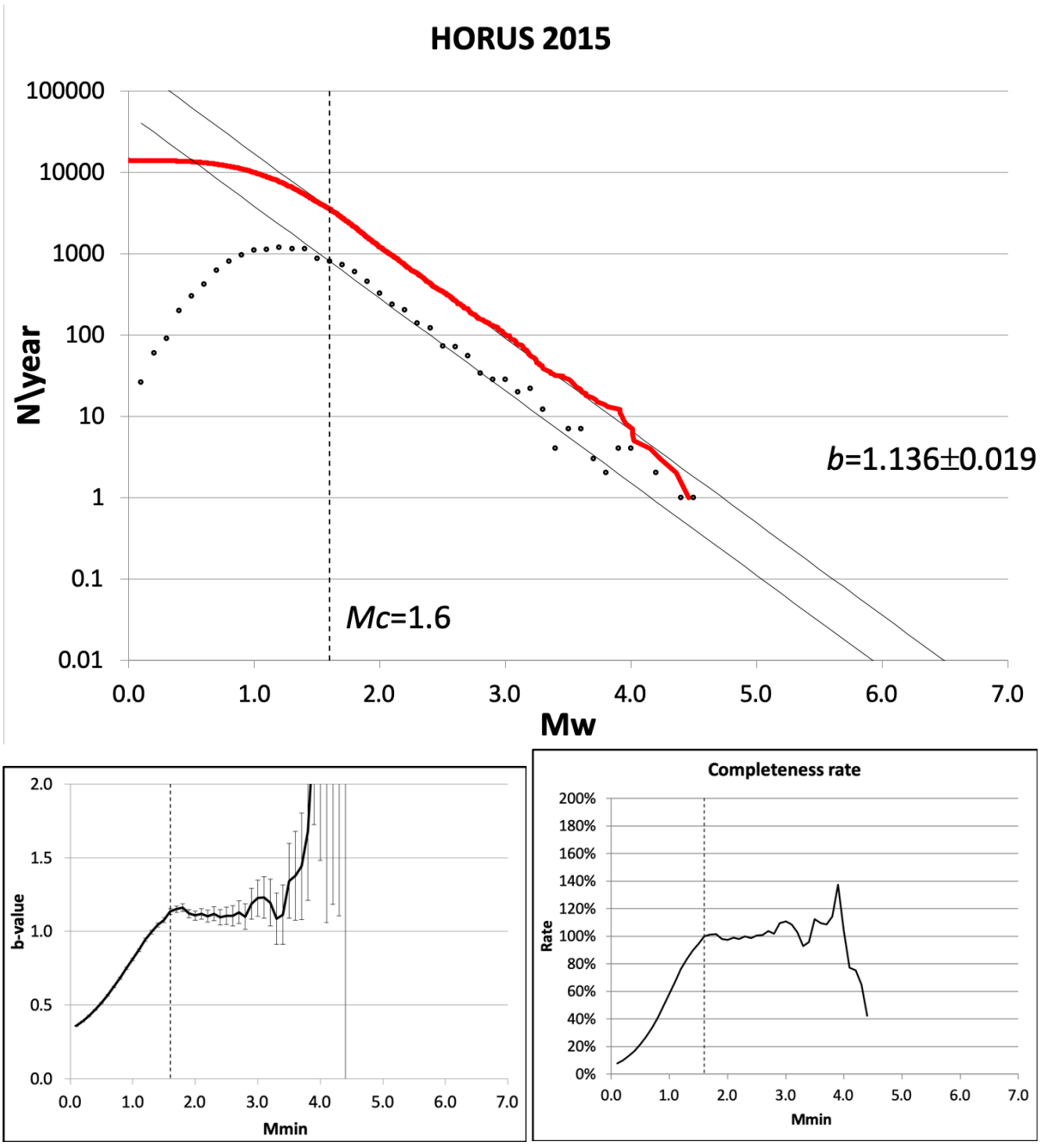

Figure S11 – Same as Fig. S1 for year 2015.

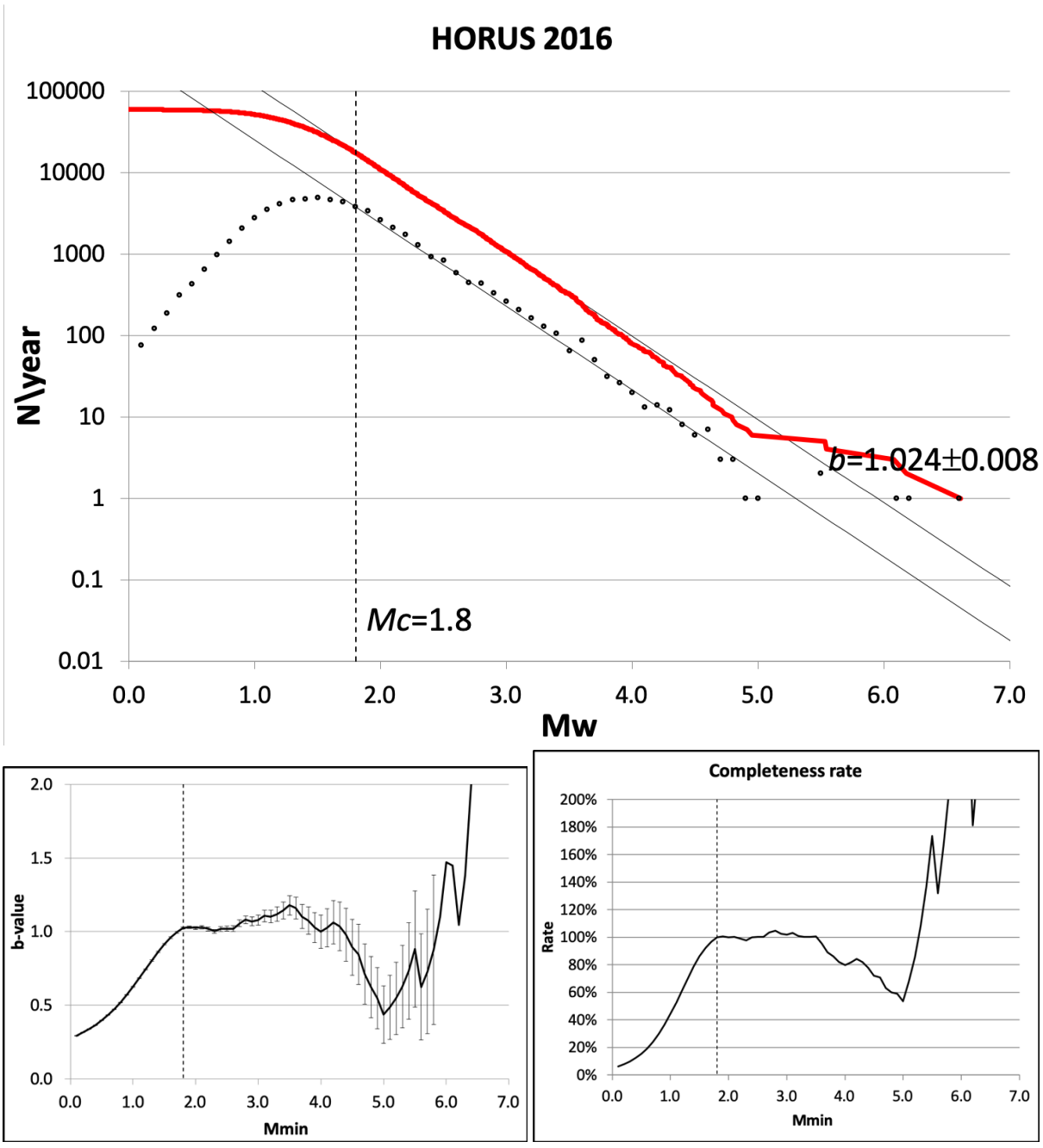

Figure S12 – Same as Fig. S1 for year 2016.

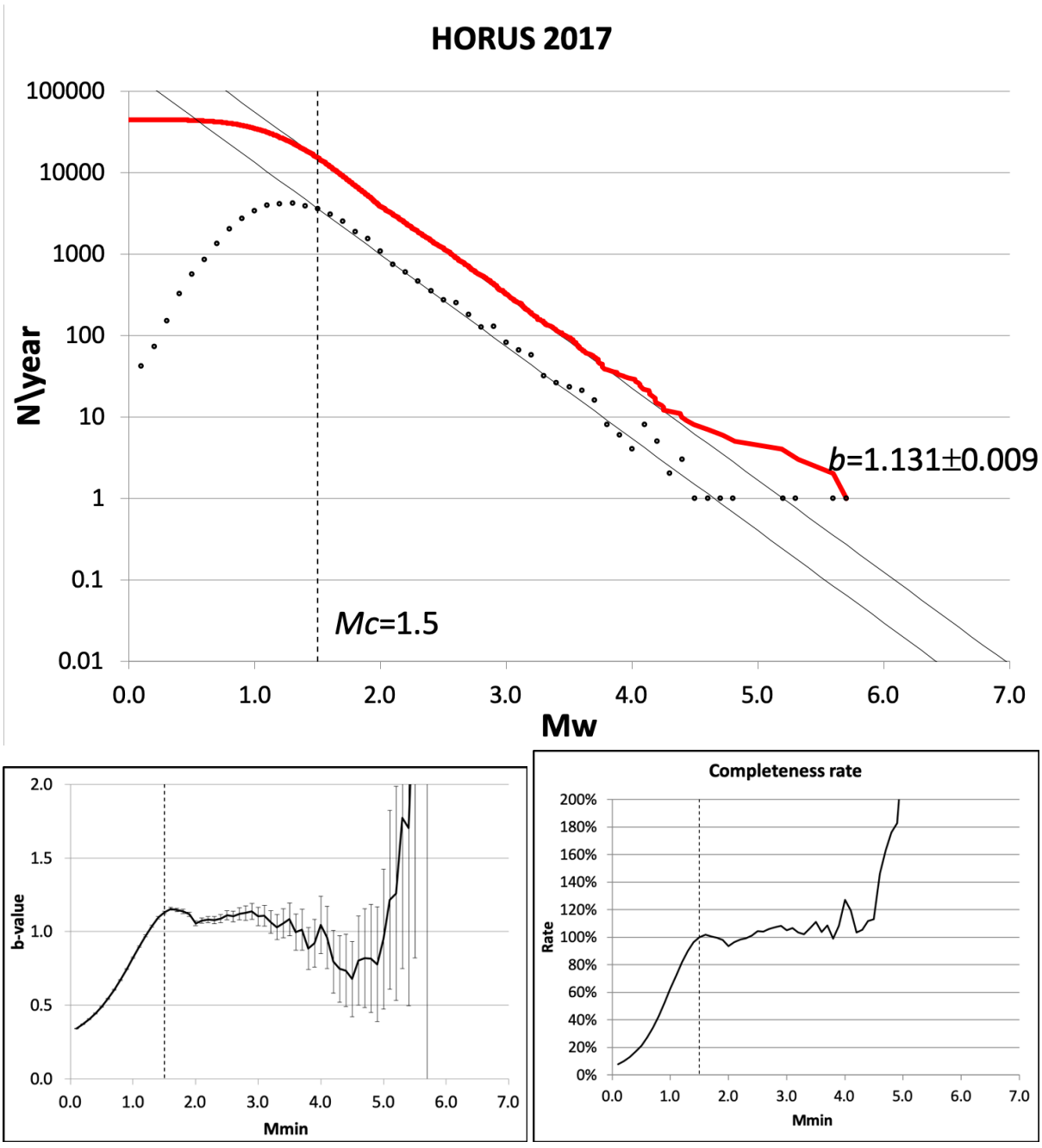

Figure S13 – Same as Fig. S1 for year 2017.

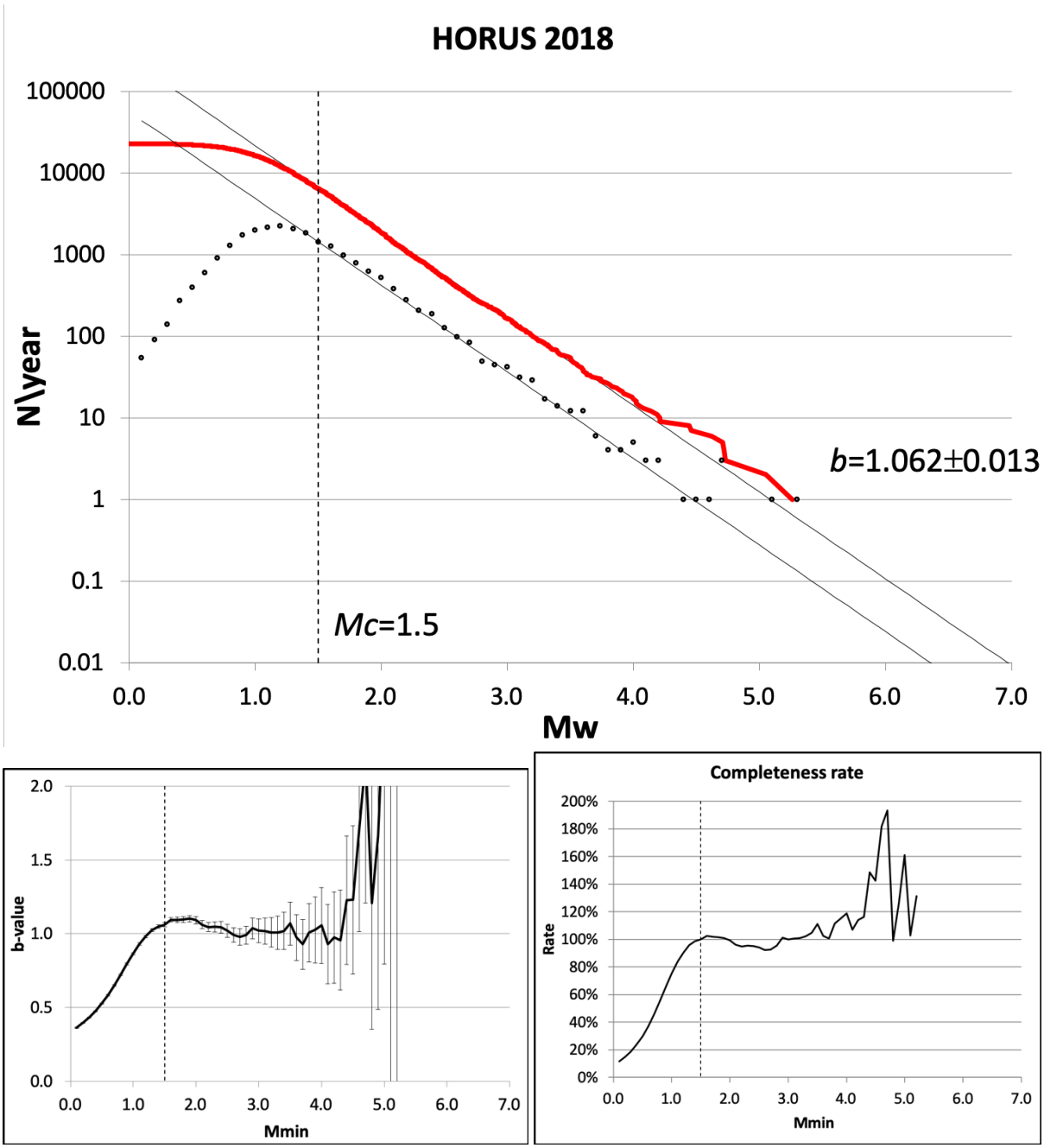

Figure S14 – Same as Fig. S1 for year 2018.

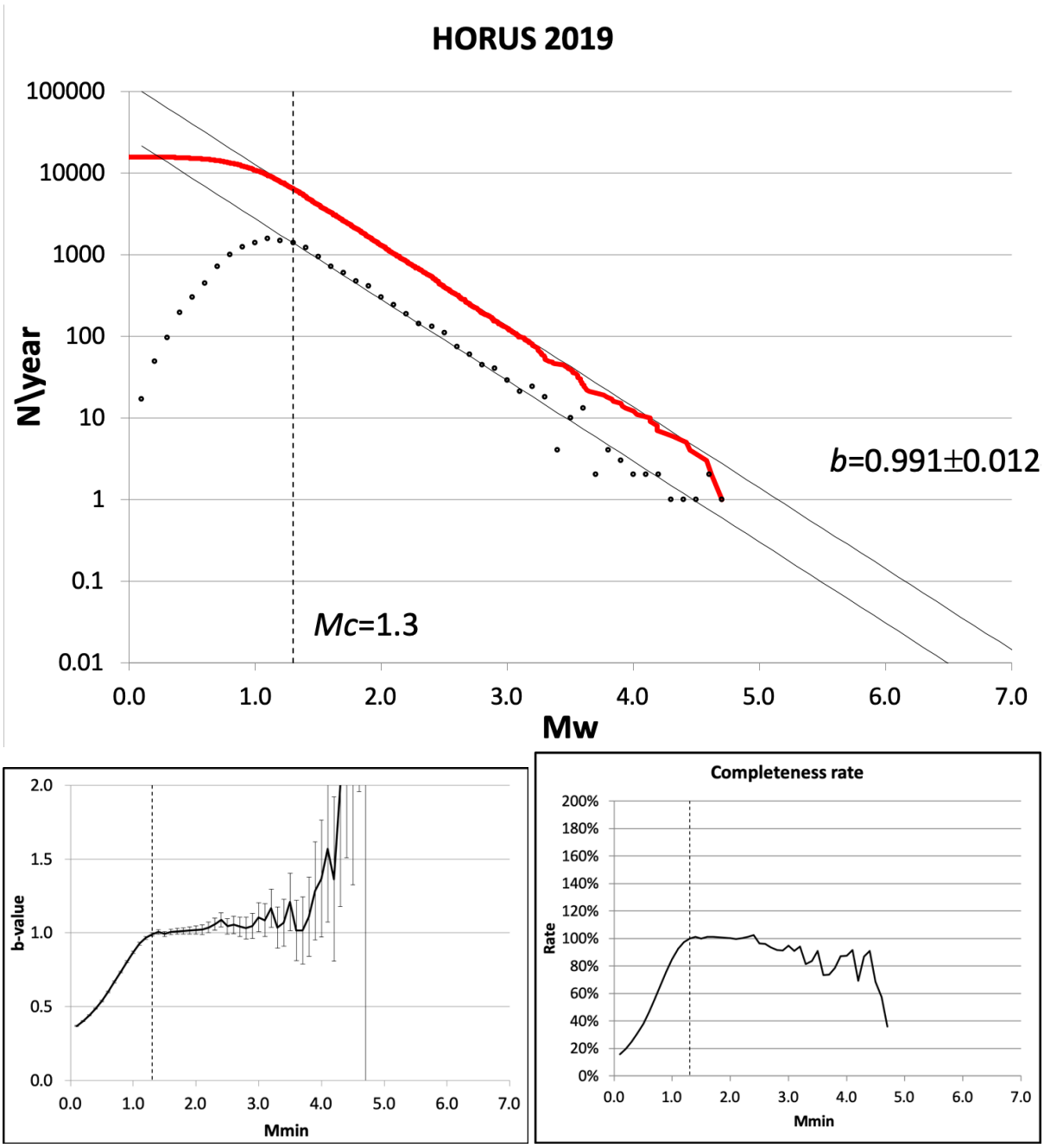

Figure S15 – Same as Fig. S1 for year 2019.

Table S1 – Average differences between ML and Md and between Mw proxies computed from ML and Md according to Gasperini et al. (2013a) with and without empirical correction to Md, in different time intervals.

Time interval	**ML_{proxy}-Md_{proxy}**	**ML_{proxy}-$(Md+0.45)_{proxy}$**	**ML-Md**
<2011	-0.002	0.772	0.459
2011	-0.030	0.743	0.506
2012	-0.169	0.604	0.387
2013	-0.800	-0.026	0.078
2014	-0.776	0.113	0.146
2015	-0.781	-0.008	0.033
2016	-0.934	-0.161	-0.063
2017	-0.670	0.103	0.227
2018	-0.689	0.013	0.248
<April 2013	-0.018	0.755	0.464
≥April 2013	-0.810	-0.038	0.080

Table S2 – Magnitude completeness thresholds, *b*-values and numbers of data in different years

Year	***Mc*(IN)**	***B*(IN)**	***Mc*(MC)**	***b* (MC)**	**N**	**$N_O \geq 2.5$**	**$N_P \geq 2.5$**
2005	1.8	0.975±0.033	1.7	0.954±0.029	2785	169	184
2006	1.7	1.026±0.024	1.6	0.991±0.021	5225	273	267
2007	1.5	1.012±0.022	1.4	0.978±0.020	5171	196	197
2008	2.0	1.025±0.032	1.6	0.925±0.020	6144	301	304
2009	1.8	0.960±0.013	1.5	0.894±0.009	25190	1201	1172
2010	1.7	1.040±0.023	1.3	0.956±0.014	13604	311	309
2011	1.5	0.977±0.015	1.2	0.886±0.010	15190	469	468
2012	2.3	0.993±0.021	1.4	0.675±0.008	16595	1365	1376
2013	1.6	1.041±0.015	1.3	0.956±0.010	23386	563	592
2014	1.7	1.134±0.019	1.3	1.033±0.011	25194	462	454
2015	1.6	1.136±0.019	1.4	1.044±0.014	14057	342	340
2016	1.8	1.024±0.008	1.7	0.995±0.007	59523	3413	3410
2017	1.5	1.131±0.009	1.5	1.131±0.009	44809	1181	1132
2018	1.5	1.062±0.013	1.4	1.049±0.012	22936	527	561
2019	1.3	0.991±0.012	1.3	0.991±0.012	15717	405	420
2005-2019	1.8	1.017±0.004	1.4	0.924±0.003	295526	11178	11105

Mc(IN) and *b*(IN) are computed by the interactive method (see text). *Mc*(MC) and *b*(MC) are computed by the corrected maximum curvature methods. *N* total number of data with Mw>0, $N_O \geq 2.5$ and $N_P \geq 2.5$ annual rates of earthquakes with Mw≥2.5, observed and predicted from the GR distribution respectively.

Table S3 – Magnitude completeness thresholds, *b*-values and numbers of data for different months of year 2009.

Year	**Mc**	***b***	**Mc(MC)**	***b* (MC)**	**N**	**$N_O \geq 2.5$**	**$N_P \geq 2.5$**
Sep08	1.6	1.294±0.104	1.5	1.157±0.085	501	12	11
Oct08	1.5	0.994±0.066	1.4	0.935±0.057	570	23	23
Nov08	1.7	0.987±0.091	1.5	0.897±0.070	369	21	19
Dec08	2.2	1.240±0.102	1.9	1.055±0.063	620	58	63
Jan	1.9	1.157±0.126	1.4	0.903±0.064	392	15	17
Feb	1.8	1.255±0.132	1.2	0.942±0.055	494	13	12
Mar	1.4	0.854±0.054	1.3	0.831±0.049	591	27	28
Apr	1.9	0.957±0.019	1.5	0.844±0.012	8940	714	694
May	1.3	1.089±0.028	1.3	1.089±0.028	3857	68	75
Jun	1.4	1.033±0.034	1.3	0.997±0.030	2645	64	66
Jul	1.7	1.055±0.054	1.3	1.016±0.033	2615	52	54
Aug	1.3	1.029±0.040	1.4	1.033±0.045	1758	42	39
Sep	1.3	1.018±0.047	1.4	1.023±0.052	1089	29	29
Oct	1.4	0.969±0.047	1.4	0.969±0.047	1255	34	37
Nov	1.5	1.041±0.067	1.3	0.960±0.051	906	23	22
Dec	2.5	1.124±0.103	1.5	0.561±0.030	648	120	120
Jan10	1.5	0.888±0.055	1.5	0.888±0.055	600	34	33
Feb10	1.8	1.086±0.100	1.6	1.009±0.076	483	23	20
Mar10	1.5	1.075±0.071	1.2	0.936±0.047	785	21	19
Apr10	1.5	1.066±0.058	1.0	0.902±0.030	1851	28	29
2009	1.8	0.960±0.013	1.5	0.894±0.009	25190	1201	1172

Mc(IN) and *b(*IN) are computed by the interactive method (see text). Mc(MC) and *b*(MC) are computed by the corrected maximum curvature methods. N total number of data with Mw>0, $N_O \geq 2.5$ and $N_P \geq 2.5$ annual rates of earthquakes with Mw≥2.5, observed and predicted from the GR distribution respectively.

Table S4 – Magnitude completeness thresholds, *b*values and numbers of data for different months of year 2012.

Year	**Mc**	***b***	**Mc(MC)**	***b* (MC)**	**N**	**$N_O \geq 2.5$**	**$N_P \geq 2.5$**
Sep11	1.8	0.881±0.053	1.3	0.741±0.031	1120	72	67
Oct11	1.5	0.883±0.045	1.4	0.849±0.040	952	52	50
Nov11	1.5	1.127±0.063	1.3	0.993±0.047	1052	26	24
Dec11	1.8	1.066±0.074	1.4	0.881±0.043	1198	37	38
Jan	1.3	0.804±0.042	1.4	0.829±0.046	864	37	40
Feb	1.5	0.902±0.064	1.4	0.885±0.057	541	24	25
Mar	1.2	0.859±0.041	1.5	0.864±0.056	807	38	33
Apr	1.3	0.975±0.048	1.2	0.944±0.043	966	34	27
May	2.3	0.893±0.027	2.6	0.840±0.036	2660	694	704
Jun	2.2	1.145±0.054	2.4	1.195±0.072	2018	200	204
Jul	1.8	1.002±0.062	1.4	0.839±0.037	1252	56	53
Aug	1.5	1.030±0.051	1.5	1.030±0.051	1380	28	38
Sep	1.5	0.975±0.046	1.4	0.949±0.041	1342	46	47
Oct	1.7	1.029±0.047	1.4	0.905±0.031	2015	74	73
Nov	1.3	0.849±0.029	1.5	0.869±0.035	1651	89	85
Dec	1.6	1.047±0.053	1.6	1.047±0.053	1099	45	44
Jan13	1.9	1.330±0.093	1.4	1.046±0.041	1270	31	33
Feb13	1.6	1.071±0.058	1.5	1.039±0.051	962	27	37
Mar13	1.6	0.979±0.058	1.6	0.979±0.058	1021	35	38
Apr10	1.4	1.000±0.042	1.1	0.910±0.029	2252	43	45
2012	1.8	0.993±0.021	1.4	0.675±0.008	16595	1365	1376

Mc(IN) and *b(*IN) are computed by the interactive method (see text). Mc(MC) and *b*(MC) are computed by the corrected maximum curvature methods. N total number of data with Mw>0, $N_O \geq 2.5$ and $N_P \geq 2.5$ annual rates of earthquakes with Mw≥2.5, observed and predicted from the GR distribution respectively.

Table S5 – Magnitude completeness thresholds, *b*values and numbers of data for different months of year 2016.

Year	**Mc**	***b***	**Mc(MC)**	***b* (MC)**	**N**	**N_O≥2.5**	**N_P≥2.5**
Sep15	1.6	1.193±0.074	1.4	1.093±0.055	1156	18	22
Oct15	1.6	1.141±0.072	1.1	0.839±0.035	930	24	24
Nov15	1.5	1.205±0.071	1.3	1.058±0.051	927	22	18
Dec15	1.3	1.072±0.055	1.5	1.065±0.070	962	21	20
Jan	2.0	1.198±0.096	1.4	0.912±0.041	1021	38	39
Feb	1.7	1.180±0.080	1.7	1.180±0.080	700	25	25
Mar	1.5	1.056±0.061	1.2	0.917±0.041	898	26	26
Apr	1.5	1.031±0.064	1.4	1.009±0.057	946	26	24
May	1.6	1.078±0.068	1.2	0.913±0.039	1041	27	27
Jun	1.5	1.060±0.062	1.4	1.012±0.053	1038	22	26
Jul	1.5	1.047±0.072	1.4	0.961±0.061	958	20	19
Aug	2.1	0.953±0.025	1.7	0.871±0.016	7084	585	595
Sep	1.7	1.255±0.028	1.4	1.152±0.018	10505	201	197
Oct	3.1	1.071±0.054	1.6	0.726±00.01	11265	1309	1735
Nov	1.9	1.228±0.018	1.9	1.228±0.018	13421	875	882
Dec	1.6	1.320±0.021	1.6	1.320±0.021	10646	259	246
Jan17	1.6	1.067±0.016	1.7	1.079±0.018	10062	489	484
Feb17	1.6	1.284±0.031	1.5	1.260±0.027	6090	134	119
Mar17	1.4	1.305±0.029	1.5	1.333±0.034	4888	75	74
Apr17	1.4	1.141±0.028	1.5	1.154±0.032	4032	114	90
2016	1.8	1.024±0.008	1.7	0.995±0.007	59507	2978	2976

Mc and b are computed by the interactive method (see text). Mc(MC) and b(MC) are computed by the corrected maximum curvature methods. *N* total number of data with Mw>0, N_O≥2.5 and N_P≥2.5 annual rates of data with Mw≥2.5, observed and predicted from the GR distribution respectively.